Environmental and biological controls on Na/Ca ratios in scleractinian cold-water corals

Nicolai Schleinkofer[1,2], Jacek Raddatz[1,2], André Freiwald[3,4], David Evans[1,2], Lydia Beuck[3], Andres Rüggeberg[4], Volker Liebetrau[5]

[1]Institute of Geosciences, Goethe University Frankfurt, Altenhöferallee 1, 60438 Frankfurt am Main, Germany

[2]Frankfurt Isotope and Element Research Center (FIERCE), Goethe University Frankfurt, Altenhöferallee 1, 60438 Frankfurt am Main, Germany

[3]Senckenberg am M0eer, Marine Research Department, Südstrand 40, 26382 Wilhelmshaven, Germany

[4]MARUM (Zentrum für Marine Umweltwissenschaften), Bremen University, Leobener Str. 8, 28359 Bremen, Germany

[5]Department of Geosciences, Faculty of Science and Medicine, University of Fribourg, Chemin du Musée 6, CH-1700 Fribourg, Switzerland

[6]GEOMAR Helmholtz Centre for Ocean Research Kiel, Wischhofstr. 1-3, D-24148 Kiel, Germany

Correspondence to: Nicolai Schleinkofer (schleinkofer@em.uni-frankfurt.de)

Abstract

Here we present a comprehensive attempt to correlate aragonitic Na/Ca ratios from *Desmophyllum pertusum* (formerly known as *Lophelia pertusa*)*, Madrepora oculata* and a caryophylliid cold-water coral (CWC) specie*s* with different seawater parameters such as temperature, salinity and pH. Living CWC specimens were collected from 16 different locations and analyzed for their Na/Ca ratios using solution-based inductively coupled plasma-optical emission spectrometry (ICP-OES) measurements.

The results reveal no apparent correlation with salinity (30.1–40.57 g/kg), but a significant inverse correlation with temperature (-0.31 ± 0.04 mmol/mol/°C). Other marine aragonitic organisms such as *Mytilus edulis* (inner aragonitic shell portion) and *Porites* sp. exhibit similar results highlighting the consistency of the calculated CWC regressions. Corresponding Na/Mg ratios show a similar temperature sensitivity to Na/Ca ratios, but the combination of two ratios appear to reduce the impact of vital effects and domain-dependent geochemical variation. The high degree of scatter and elemental heterogeneities between the different skeletal features in both Na/Ca and Na/Mg however limit the use of these ratios as a proxy and/or make a high number of samples necessary. Additionally, we explore two models to explain the observed temperature sensitivity of Na/Ca ratios for an open and semi-enclosed calcifying space based on temperature sensitive Na and Ca pumping enzymes and transport proteins that change the composition of the calcifying fluid and consequently the skeletal Na/Ca ratio.

1. Introduction

Sodium to calcium ratios (Na/Ca) has been proposed as a new tool in paleoceanography to reconstruct seawater salinities. Cultured benthic and planktonic foraminifera as well as living planktonic foraminifera from the Red Sea showed the potential of calcitic Na/Ca ratios as an salinity proxy (Mezger et al., 2016; Wit et al., 2013). Cold-water corals provide one of the most promising marine paleoenvironmental archives for climatic research due to the potential to reconstruct high-resolution records using the aragonitic skeleton (Druffel, 1997). About half of the known scleractinian coral species do not live in tropical, shallow water (<50 m) but in

deeper waters, including deep-sea environments (>200 m) (Roberts et al., 2009). These deep

or cold-water corals lack phototrophic symbionts and therefore are azooxanthellate. Like their

zooxanthellate shallow-water relatives, some azooxanthellate deep water species, such as

Desmophyllum pertusum and *Madrepora oculata,* are also capable of building large three-

dimensional reef frameworks that serve as habitats for thousands of different organisms and

constitute biodiversity hotspots in low to high latitudes and from shallower water to the deep

seas (Henry and Roberts, 2016; Roberts et al., 2009). The distribution of CWC is controlled by

several parameters, amongst which is the density of seawater (Dullo et al., 2008) which

appears to correlate with the so called Intermediate Nepheloid Layers (INL). These INL

contribute an important source of particulate organic matter (POM) (Kiriakoulakis et al., 2005,

2007) that CWC feed on. Additionally, it has been suggested, that gamete density restricts the

lateral transport to certain density envelopes (Dullo et al., 2008). For *D. pertusum*, the suitable

density envelope amounts to σ_θ = 27.35–27.65 kg/m^3 (Dullo et al., 2008), although these

values are not applicable to every oceanic region (Flögel et al., 2014; Freiwald et al., 2009;

Rüggeberg et al., 2011). Since seawater density is a function of temperature and salinity, these

parameters also partly control the spatial distribution of CWC. Most known CWC occur in

salinities of 35 g/kg and mean temperatures of 4–12°C (Freiwald, 2002; Freiwald and Roberts,

2005), although they are also able to thrive in lower and higher temperatures and salinities

(e.g. Bett, 2001; Roder et al., 2013; Taviani et al., 2005).

Independent proxies are needed to reconstruct the environment in which CWC lived in the past

to better understand their temperature/salinity/pH tolerances and to study the influence of

parameters on their spatial distribution. This would also help to better locate new unknown

sites of CWC occurrences. For temperature and pH, different geochemical proxies can be used

to calculate these parameters in the geological past. Sr/Ca and Li/Mg ratios serve as

temperature proxies (Cohen et al., 2006; Gagnon et al., 2007; Mitsuguchi et al., 1996;

Montagna et al., 2014; Raddatz et al., 2013, 2014a; Rollion-Bard and Blamart, 2015; Shirai et

al., 2005), U/Ca and Boron-isotopes serve as proxies of the carbonate system(Anagnostou et

al., 2011, 2012; Blamart et al., 2007; McCulloch et al., 2012; Raddatz et al., 2014b, 2016;

74   Rollion-Bard et al., 2011). However, independent geochemical methods to reconstruct past

75   salinities are absent but urgently needed to reconstruct spatial distribution patterns in the past

76   and quantify effects of ocean acidification on CWC by researching its effects in the past. Even

77   though CWC show that they can maintain growth in under-saturated, corrosive waters, the

78   older unprotected parts of the reef are susceptible for dissolution (Büscher et al., 2017; Form

79   and Riebesell, 2012).This weakens the reef integrity and might cause severe implications on

80   available microhabitats (Büscher et al., 2017; Roberts, 2006)

81   Reconstructing past salinities can be accomplished with several different techniques, e.g.

82   diatom and dinoflagellate species composition(Zonneveld et al., 2001), morphology and size

83   of placoliths from *Emiliana huxleyi* (Bollmann et al., 2009)*,* Ba/Ca ratios in foraminiferal calcite

84   (Weldeab et al., 2007), the strontium isotope composition of bivalves (Israelson and Buchardt,

85   1999), process length of dinoflagellate cysts (Mertens et al., 2009), hydrogen isotope

86   composition of alkenones (van der Meer et al., 2007; Schouten et al., 2006) or temperature

87   corrected (Mg/Ca, TEX_{86}) oxygen isotopes (Elderfield and Ganssen, 2000). While some of

88   these proxies may yield reliable results (e.g. coupled Mg/Ca and oxygen isotopes (Elderfield

89   et al., 2012; Lear et al., 2000)) others suffer from rather large uncertainties introduced by

90   modelled parameters or require a good knowledge of the regional oceanography (Wit et al.,

91   2013). Others, like Ba/Ca ratios are more effected by terrestrial runoff and are therefore only

92   applicable in proximal sites. Complications with the existing proxies mean that further methods

93   are desirable, therefore we explore here whether coral Na/Ca ratios may be useful in this

94   regard.

95   The influence of seawater salinity on Na/Ca ratios are known from Atlantic oysters (Rucker

96   and Valentine, 1961), barnacle shells (Gordon et al., 1970) as well as inorganically precipitated

97   calcium carbonate (Ishikawa and Ichikuni, 1984). Recently it has been shown that Na

98   incorporation in calcitic planktonic and benthic foraminifera appears to be at least partly

99   controlled by seawater salinity (Allen et al., 2016 (only in *Globigerinoides ruber*); Mezger et al.,

100 2016; Wit et al., 2013). According to Wit et al. (2013), the incorporation of Na in calcite depends

on the activity of Na in the seawater which is a function of salinity. There is strong evidence that Na substitutes for Ca in biogenic aragonite despite its charge difference (Okumura and Kitano, 1986; Yoshimura et al., 2017). However, since Na and Ca compete for the same lattice positions, the calcium concentration and Na/Ca activity ratio of the surrounding seawater might also control the amount of sodium incorporation (Ishikawa and Ichikuni, 1984; White, 1977). Over longer periods of geological time, when concentrations of some elements in seawater have varied, this would inhibit the use of Na/Ca ratios as a salinity proxy but might prove useful to reconstruct oceanic calcium concentrations. Recent studies also show that the Na/Ca ratio in foraminiferal calcite is also mainly controlled by seawater Na/Ca ratios (Hauzer et al., 2018).

In this study, we investigate the impact of different seawater parameters on the incorporation of Na in the aragonitic skeleton of the scleractinian cold-water coral *D. pertusum, M. oculata* and a caryophylliid species from the Red Sea. The corals were collected alive from a variety of locations to cover a broad range of temperatures (5.9–21.6°C) and salinities (30.1–40.6 g/kg).

2. Materials & Methods

2.1. Study area and sample collection

The samples were taken from 45 different coral specimens collected from 16 different locations (Tab. 1). Most of the samples (n=25) were collected during different cruises from the Norwegian margin. The other samples derive from the Irish Margin and Bay of Biscay (n=4), the Mediterranean Sea and Gulf of Cadiz (n=7), the Gulf of Mexico and Great Bahama Bank (n=4) and the Red Sea (n=5) (Fig. 1). Conductivity-Temperature-Depth (CTD) downcast data for water parameters was available for all locations except the Red Sea and the Gulf of Mexico. Where no CTD data was available, the water parameters were retrieved from annual averaged data from World Ocean Atlas 2013 (Locarnini et al., 2013; Zweng et al., 2013). Where available, comparison of *in-situ* CTD and WOA13 data, revealed an agreement within 0.15°C in Santa Maria de Leuca and 0.04°C in the Bay of Biscay respectively. The seawater carbonate system data such as pH was taken from the associated cruise report (Flögel et al., 2014) or in

128 case of the Red Sea and the western Atlantic from Mezger et al., (2016) and CARINA. Flögel

129 et al., 2014 used a WTW Multi 350i compact precision hand- held meter to determine pH

130 (Flögel et al., 2014), pH in the Red Sea was calculated from DIC and TA, measured during

131 PELAGIA 64PE158 (Mezger et al., 2016), using CO2SYS (Lewis and Wallace, 1998). pH

132 values are reported using the total scale.

133 We took 31 samples from different coral colonies and three different species (*D. pertusum, M.*

134 *oculata,* Caryophylliidae) that were collected during different cruises. The samples were taken

135 from the uppermost calices after physically cleaning them with a dental drill tool to remove

136 secondary overgrowths. We avoided further cleaning or rinsing with water because studies

137 suggest that structurally substituted Na is readily leached even by distilled water (Ragland et

138 al., 1979). It is possible that organic contents inside the skeleton bias the results as shown in

139 foraminifera (Branson et al., 2016). However, the study on foraminifera shows that the Na/Ca

140 ratio only significantly varies at POS (primary organic sheet) regions. In corals the COC

141 (centers of calcification) would be an equivalent structure, which we avoided during the

142 sampling process. Furthermore, it has been suggested that these regions only significantly

143 affect bulk sample elemental ratios in very thin-walled foraminifera (Branson et al., 2016). In

144 corals the area of COC is larger (20% of the total skeleton radius (Rollion-Bard and Blamart,

145 2015)) but the Na/Ca ratio does not increase in the COC as strong as it does in the POS areas

146 of foraminifera (Branson et al., 2016; Rollion-Bard and Blamart, 2015). Avoiding the COC areas

147 in bulk samples only reduces the mean Na/Ca ratio by 0.18 mmol/mol ($0.18\,mmol/mol =$

148 $\overline{Na/Ca}_{inc.\,COC}^{Sample\,1-i} - \overline{Na/Ca}_{exc.\,COC}^{Sample\,1-i}$), additional cleaning of organic material is therefore not

149 necessary. An additional 14 samples (*D. pertusum*) were prepared as longitudinal slices

150 through the coral's calice, glued on metal plates. In order to identify elemental heterogenities

151 within the theca wall, subsamples were taken using a micromill (Merchantec MM-000-134).

152 **2.2. ICP-OES Analyses**

153 Elemental ratios were measured by inductively coupled plasma optical emission spectrometry

154 (ICP-OES). The ICP-OES analysis was carried out with a Thermoscientific iCap 6300 dual

viewing at Goethe University/Frankfurt. This machine is both capable of measuring axially and radially. Alkali metals (Na) were measured radially on line 589.59 nm whereas earth-alkali metals (Mg, Sr) were measured axially on lines 279.55 nm and 421.55 nm respectively. The sample powder ($\approx$ 140 µg) was dissolved in 500 µl HNO_3 (2%) and 300 µl aliquots were separated. Subsequently 1500 µl of 1.2 mg/l yttrium solution was added to each aliquot as an internal standard resulting in 1 mg/l. The intensity data was background subtracted and standardized internally to Y and normalized to Ca. External standards were mixed from single element standard solutions to match the typical element concentrations of cold-water corals (cf. Rosenthal et al., 1988). The coral standard JCp-1 (Hathorne et al., 2013; Okai et al., 2002) was measured after every tenth sample to allow for drift correction and monitor measurement quality.

Relative precision of the Element/Ca measurements was based on the international calcium-carbonate standard JCp-1 (20 replicates) and amounts to 20.47 ± 0.68 mmol/mol Na/Ca (19.8 ± 0.14 mmol/mol (Okai et al., 2002)), 4.09 ± 0.11 mmol/mol Mg/Ca (4.199 ± 0.065 mmol/mol (Hathorne et al., 2013; Okai et al., 2002)) and 9.36 ± 0.07 mmol/mol Sr/Ca (8.838 ± 0.042 mmol/mol (Hathorne et al., 2013; Okai et al., 2002)). Measurements were conducted in two sessions lasting ten and five hours.

2.3. Data Processing

Before calculations of correlations or applying statistics outliers were removed from the raw data. Outliers were identified by the average ±1.5 SD per oceanic region (Norwegian margin, Bay of Biscay/Irish Margin, Mediterranean Sea, Red Sea, Gulf of Mexico/Bahamas). The threshold was chosen to eliminate data points <15 mmol/mol and >35 mmol/mol cover a range from 15 to 35 mmol/mol which is roughly 5 mmol/mol higher and lower than the reported range from a similar study (Rollion-Bard and Blamart, 2015). The profiled samples were additionally checked for values that derive from the COC, which are identifiable through a positively correlating increase in Mg/Ca and Na/Ca. The chosen threshold was the mean of the profiled

181   sample + 2SD of JCp-1. Statistical calculations were conducted with the ORIGIN Pro software

182   suite.

3. Results

184   Spatial distribution patterns show great variations in Na/Ca ratios through the corals skeleton

185   (Fig. 2). In the COC and COC-like structures (structures that geochemically correspond to

186   COC but morphologically to fibrous deposits) Na/Ca ratios show significant increases but the

187   amount of increase relative to the mean is not uniform in the sample. Increases range from +2

188   to +10 mmol/mol. Mg/Ca is positively correlated with Na/Ca in the COC structures but mostly

189   independent from each other in the fibrous deposits (FD). Similar to Na/Ca, the amplitude of

190   Mg/Ca in the COC-structures is very variable in their amount and ranges from +0.5 to +3

191   mmol/mol. Both sodium and magnesium are often enriched in the outermost parts of the theca.

192   Sr/Ca ratios are mostly stable throughout the theca and seem to be independent from the

193   different skeletal structures. In some samples, co-variances between Sr/Ca and Mg/Ca;Na/Ca

194   are present but in general they do not appear to be controlled by the skeletal morphology in

195   the same way as Mg/Ca and Na/Ca as shown by their independency from the different skeletal

196   structures.

3.1 Element/Ca ratios of scleractinian cold-water corals

198   Na/Ca ratios vary between 20.49 ± 1.36 (1SD) mmol/mol in the Red Sea and 31.04 ± 1.36

199   mmol/mol in the Norwegian reefs with a mean at 25.22 mmol/mol and a standard deviation of

200   2.8 mmol/mol (Fig. 3). The values are in accordance to previous studies on *D. pertusum*

201   (21.94–28.11 mmol/mol (Rollion-Bard and Blamart, 2015)), but 5 mmol/mol higher than

202   reported for zooxanthellate corals (Amiel et al., 1973; Busenberg and Niel Plummer, 1985;

203   Mitsuguchi et al., 2001; Ramos et al., 2004; Swart, 1981). Significant deviations between *D.*

204   *pertusum (n=38)*, *M. oculata* (n=2) and Caryophylliidae (n=5) are not observable. A linear

205   correlation between salinity and Na/Ca over the whole salinity range is not observable, but the

206   present dataset is best described with a second order polynomial function. Accordingly, there

207   is a positive trend from 30.1–35 g/kg followed by a negative trend from 35–40.5 g/kg. Linear

208 regressions equal: $f(S_{30.1-35}) = 6.4 + 0.56 * S$ ($R^2 = 0.99$, $P = 0.072$) and $f(S_{35-40.5}) = 56.61 -$

209 $0.84 * S$ ($R^2 = 0.66$, $P = 0.4$). As the P-values show a significant slope is missing in all these

210 regressions. In the case of the polynomial fit the P-value shows that the fit is not significantly

211 superior to $f(S_{30,1-40,5}) = $ constant.

212 Na/Ca and temperature show a significant negative correlation, which is however mainly driven

213 by the samples from the highest temperature (Red Sea). The linear regression equals:

214 $$f_{T\,6-22°C} = 28.2 \pm 0.9 - 0.31 \pm 0.07 \times T\ (R^2 = 0.87, P = 0.02) \tag{1}$$

215 Temperature and salinity show a positive correlation, accordingly this negative correlation

216 cannot be caused by covariances between salinity and temperature. Corals from the

217 Mediterranean Sea are slightly elevated in their Na/Ca ratio, but within error they still fit the

218 correlation with both salinity and temperature. Distribution coefficients ($K_d^{Na} = $ Na/Ca$_{carbonate}$/

219 Na/Ca$_{seawater}$) at specific temperatures for several different species, including the scleractinian

220 cold-water corals from this study, *Porites* sp. and *M. edulis*, show similar values. K_d^{Na} from this

221 study amounts to $K_d^{Na}{}_{(6.2°C)} = 5.73*10^{-4}$, $K_d^{Na}{}_{(7.9°C)} = 5.51*10^{-4}$, $K_d^{Na}{}_{(9.8°C)} = 5.44*10^{-4}$, $K_d^{Na}{}_{(13.5°C)}$

222 $= 5.62*10^{-4}$, $K_d^{Na}{}_{(21.6°C)} = 4.73*10^{-4}$. Distribution coefficients for *Porites* sp. and *M. edulis* are

223 $K_d^{Na}{}_{(26.03°C)} = 4.6*10^{-4}$ (Mitsuguchi et al., 2001) and $K_d^{Na}{}_{(12.5°C)} = 5.25*10^{-4}$ (Lorens and Bender,

224 1980) respectively. For comparison, the inorganic distribution coefficient is with $4.00*10^{-4}$ at

225 15°C, about 20% lower (Kinsman, 1970). The results from White (1977) show that the

226 composition of the solution affects the elemental ratios in the precipitate, but in the study from

227 Kinsman (1970) the precipitation happened from seawater. Therefore, it is reasonable to use

228 this data for comparison. A combined regression using the data from this study, the *D.*

229 *pertusum* data from Rollion-Bard and Blamart (2015), *M. edulis* data from Lorens and Bender

230 (1980) and *Porites* sp. data from Ramos et al. (2004) and Mitsuguchi et al. (2001) equals:

231 $$f_{T\,6-27.63\,°C} = 28.03 \pm 0.7 - 0.31 \pm 0.04 \times T\ (R^2 = 0.9, P < 0.0001) \tag{2.}$$

232   Na/Ca also shows a significant positive correlation with pH of the ambient seawater. Linear

233   regression equals: f(pH) = - 84.26 ± 40.15 + 13.63 ± 5.49 * pH (R^2 = 0.14, P= 0.017). A negative

234   trend between pH and temperature is visible.

235   **3.2. Mg/Ca & Sr/Ca**

236   Mg/Ca values vary between 2.2 ± 0.2 mmol/mol in the Red Sea and 6.38 ± 0.2 mmol/mol in

237   the Mediterranean Sea with a mean of 3.99 mmol/mol and a standard deviation of 0.97

238   mmol/mol (Fig. 4). Maximum values are higher than literature states for *D. pertusum* (2.99–

239   4.72 mmol/mol (Cohen et al., 2006; Gagnon et al., 2007; Raddatz et al., 2013; Rollion-Bard

240   and Blamart, 2015)) but the mean values are well inside the range of literature. Significant

241   deviations between *D. pertusum*, *M. oculata* and Caryophylliidae are not observable, although

242   there are limited published data *M. oculata* and Caryophylliidae. Seawater parameters such

243   as temperature, salinity and pH have no significant effect on Mg/Ca ratios in the skeleton.

244   Sr/Ca values vary between 9.46 ± 0.14 and 10.46 ± 0.14 mmol/mol with a mean of 10.1 ± 0.14

245   mmol/mol and a standard deviation of 0.25 mmol/mol (Fig. 5). Both maximum and minimum

246   values derive from corals that grew in reefs that are located in the Trondheimfjord. The values

247   are in accordance to previous studies on *D. pertusum* (9.27–10.05 mmol /mol (Cohen et al.,

248   2006; Gagnon et al., 2007; Raddatz et al., 2013)). Significant deviations between *D. pertusum*,

249   *M. oculata* and Caryophylliidae are not observable. Despite the known temperature effect on

250   Sr/Ca ratios this effect is not pronounced in this dataset. The correlation shows a strongly

251   deviating slope of -0.015 mmol/mol/°C in comparison to that given in literature (-0.083 ± 0.017

252   mmol/mol/°C (Raddatz et al., 2013)). Linear regressions equal: f(T) = 10.26 ± 0.05 − 0.015 ±

253   0.004 * T (R^2 = 0.83, P = 0.03). Sr/Ca vs. salinity values show a distribution pattern similar to

254   that of Na/Ca vs. salinity values with the maximum at 35 g/kg and descending values at lower

255   and higher salinities but an AIC and a F-Test confirm that a linear fit is better suited. The Linear

256   regression equals f(S) = 10.58 ± 0.03 − 0.015 ± 0.01 * S (R^2 = 0.52, P = 0.17). *P*-values show

257   that the correlation is not significant.

258   **3.3 Element concentrations in the extracellular calcifying fluid (ECF)**

259   Based on the assumption of a semi-enclosed ECF with seawater-leakage and a consequent

260      $[Na]_{ECF}$ similar to $[Na]_{Seawater}$ it is possible to calculate $[Ca]_{ECF}$ and $[Mg]_{ECF}$ using skeletal Na/Ca

261   and Mg/Ca data. Assuming $[Na]_{Seawater}$ = $[Na]_{ECF}$ = 455 mmol/l (Turekian et al., 2010) and an

262   invariant Na distribution coefficient, $[Ca]_{ECF}$ can be calculated with the following equation:

263      $$[Ca]_{ECF} = [Na]_{ECF} * \frac{K_d^{Na}}{\frac{Na}{Ca}_{Coral}}$$ (3)

264   In order to do so, knowledge of K_d^{Na} is required. White (1977) reports 1.8 – 4.1*10^{-4} for inorganic

265   aragonite in the four experiments with solution Na/Ca closest to the natural seawater ratio (~45

266   mol/mol), which would result in predicted aragonite Na/Ca ratios of 8 – 18 mmol/mol, slightly

267   lower than the coral aragonite values we measure. Because this difference may be explained

268   via differences in (e.g.) inorganic and coral aragonite growth rates (Mucci, 1988; White, 1977;

269   Yoshimura et al., 2017) or the presence of organics (Amiel et al., 1973; Cuif et al., 2003;

270   Stolarski, 2003), we adjust our data so that the predicted aragonite Na/Ca ratios fit our

271   measured ratios by using K_d^{Na}=5.37*10^{-4} calculated from the coral samples presented here.

272   As such we cannot presently constrain absolute $[Ca]_{ECF}$ values using this method, however the

273   aim here is simply to explore whether differences in $[Ca]_{ECF}$ can explain the variance in both

274   our Na/Ca and Mg/Ca data. An improved understanding of the inorganic distribution coefficient

275   may enable both precise and accurate ECF reconstructions in the future. Using the method

276   outlined above, we calculate $[Ca]_{ECF}$ values ranging from 7.9 mmol/l to 12.3 mmol/l with a mean

277   of 9.9 mmol/l. This range is in good agreement with the microsensor studies on *Galaxea*

278   *fascicularis* conducted by Al-Horani et al., (2003)(9-11 mmol/l). By substituting these data into

279   the equation:

280      $$[Mg]_{ECF} = \frac{Mg}{Ca}_{Coral} * \frac{[Ca]_{ECF}}{K_d^{Mg}}$$ (4)

281   With K_d^{Mg}=7.9*10^{-4}, calculated from the coral samples presented here, $[Mg]_{ECF}$ can also be

282   calculated. Resulting values range from 32.8 mmol/l to 104.7 mmol/l and a mean of 51.5 mmol/l

283   and a median of 46.5 mmol/l. Results show that the Mg-concentration in the ECF is constant

284   with changing Ca-concentration.

4. Discussion

4.1 Heterogeneities of elemental ratios in scleractinian corals

Ninety percent of the sodium in corals is located in the aragonitic mineral phase, the remaining sodium is bound to organic material and exchangeable sites (Amiel et al., 1973). Magnesium, which co-varies with sodium, is not located in the aragonitic phase but either organic material (20–30%) and a highly disordered inorganic phase such as amorphous calcium carbonate (ACC) (70–80%) (Amiel et al., 1973; Finch and Allison, 2008) or nanodomains of Mg-bearing carbonate occluded in the aragonite (Finch and Allison, 2008). A small percentage seems to be also trapped along the (001) surface (Ruiz-Hernandez et al., 2012). Elemental heterogeneities are particularly visible when comparing COC and fibrous deposits (Fig. 2). COC are both chemically and morphologically distinct from the fibrous deposits. While the COC are built by sub-micron sized granular crystals (Constantz, 1989), the fibers that build the fibrous zones are not single orthorhombic crystals but elongated composite structures with very fine organo-mineral alternations (Cuif and Dauphin, 1998). Reasons for the different chemical composition are still under debate and include: (1) pH variations in the calcifying fluid (Adkins et al., 2003; Holcomb et al., 2009), (2) Rayleigh fractionation (Cohen et al., 2006; Gagnon et al., 2007), (3) kinetic fractionation (McConnaughey, 1989; Sinclair et al., 2006), (4) mixed ion transport through direct seawater transport and ionic pumping (Gagnon et al., 2012), and (5) precipitation from different compartments (Meibom et al., 2004; Rollion-Bard et al., 2010, 2011).

The missing co-variance between Sr/Ca and Mg/Ca or Na/Ca ratios excludes Rayleigh fractionation as the main mechanism responsible for the large variances of elemental ratios (Rollion-Bard and Blamart, 2015), as well as mixed ion transport for similar reasons (Rollion-Bard and Blamart, 2015). pH variations and consequent changes in the saturation of the calcifying fluid have been shown to alter Mg/Ca ratios in corals and abiogenic aragonite (Holcomb et al., 2009) and therefore, could potentially alter Na/Ca ratios as well. While the pH-elevation at the COC is supported by several studies (McCulloch et al., 2012; Raddatz et al.,

312 2014b; Sinclair et al., 2006), Tambutté et al. (2007) propose that the nanometer-sized spaces

313 between the skeleton and the calicoblastic ectoderm does not allow a modification of the

314 saturation state. Also, studies based on $\delta^{11}B$ measurements show that the COC might be an

315 area of lower pH-values compared to the fibrous zones (Blamart et al., 2007; Jurikova et al.,

316 2019; Rollion-Bard et al., 2011). Our data may be explained by different calcification

317 compartments (Meibom et al., 2004; Rollion-Bard et al., 2010, 2011) in combination with kinetic

318 effects caused by rapid calcification rates. Additionally, we propose changing organic contents

319 as a further mechanism that controls elemental ratio differences in the different skeletal parts,

320 visible in the covariance of Mg/Ca and Na/Ca ratios throughout the skeleton. However, it is not

321 clear in what way the different precipitation regions are distinct from each other, for example

322 whether they are characterized by different cell types or different modes of the same cell types

323 (Rollion-Bard et al., 2010). So far, only calicoblasts and desmocytes are known from the aboral

324 ectoderm of corals (Allemand et al., 2011; Tambutté et al., 2007) but calicoblasts show

325 differences in their morphology, ranging from very thin, long and flat to thick and cup like

326 (Tambutté et al., 2007). A major controlling factor on the cell shape is the calcification activity,

327 with flat calicoblasts corresponding to low calcification activity and thick calicoblasts to high

328 calcification activity (Tambutté et al., 2007). These different cell morphologies might be the

329 reason for different types of precipitation, ACC, a proposed precursor phase of aragonite (Von

330 Euw et al., 2017; Rollion-Bard et al., 2010), and granular crystals in the COC regions or organo-

331 mineral fibers in the fibrous deposits. The precipitation of ACC in the COC would certainly

332 explain the enrichment of Mg in these areas, as it is necessary to stabilize the otherwise

333 unstable ACC (Von Euw et al., 2017), however, the relevance of ACC to coral calcification has

334 been questioned as it has so far not been possible to form ACC under carbonate system

335 conditions thought to characterize the calcification space (Evans et al., 2019). Alternatively ,

336 the COC are known to be rich in organic material (Cuif et al., 2003; Stolarski, 2003), which

337 would also explain the enrichment of Mg as well as explaining a slight enrichment of Na.

338 However, the amount of Na bound to organic material is not high enough (Amiel et al., 1973)

339 that the enrichment in the COC can be solely explained by high organic contents. Kinetic

effects, due to rapid calcification rates are more likely to be the main control for Na variations in COC and fibrous deposits. Since Na is incorporated in the aragonite lattice by direct substitution with Ca (Okumura and Kitano, 1986; Yoshimura et al., 2017), charge differences occur due to the exchange of divalent Ca with monovalent Na. These charge differences need to be compensated by lattice defects (CO_3^{2-} vacancies), which occur more often at higher precipitation rates (Mucci, 1988; White, 1977; Yoshimura et al., 2017). Growth rate effects are also known for the incorporation of Mg into inorganic aragonite, albeit these effects more likely result from crystal surface entrapment of Mg by new formed aragonite (Gabitov et al., 2008, 2011; Watson, 1996).

Sr/Ca ratios in the warm-water coral *Pocillopora damicornis* seems to be largely unaffected by growth rate changes over a range of one to over 50 µm/day (Brahmi et al., 2012), at least when comparing different skeletal architectures (Fig. 2). This is supported by our data as the observed Sr/Ca ratios show no significant decrease in the COC or COC-like areas as would be expected from the results of de Villiers et al. (1994) despite the significantly different growth rates in these areas (COC > 50–60 µm/day, FD = 1–3 µm/day (Brahmi et al., 2012)). In fact, an increase in the COC is more often but still not regularly visible (Cohen et al., 2006). Consequently, a significant effect of the different skeletal architectures on Sr/Ca ratios in coralline aragonite can be excluded. Slight increases in the COC however can be explained with the great adsorbtion potential of Sr to organic matter (Chen, 1997; Khani et al., 2012; Kunioka et al., 2006)

4.2. Environmental control on coral Na/Ca ratios

4.2.1. Salinity

Recently, Na/Ca ratios in foraminiferal calcite have been suggested as a potential salinity proxy (Allen et al., 2016; Bertlich et al., 2018; Mezger et al., 2016; Wit et al., 2013). Ishikawa and Ichikuni (1984) proposed that the activity of Na in seawater is the primary controlling factor for the incorporation of Na in calcite. However, more recent studies have shown that Na/Ca in foraminiferal calcite is mainly driven by the seawater Na/Ca ratio instead of the Na activity

367 when this is the dominant variable (Evans et al., 2018; Hauzer et al., 2018). Species-specific

368 offsets make further biological controls highly plausible.

369 In this study, no correlation between salinity and Na/Ca ratios is present (Fig. 3). The positive

370 trend up to 35 g/kg followed by a negative trend after 35 g/kg can be explained by growth rate

371 changes due to the changing salinity. To our knowledge no studies on the effect of salinity on

372 growth rates have been conducted on *D. pertusum* but it is plausible that it shows reduced

373 growth rates in salinities diverging from the biological optimum similar to other marine

374 organisms (e.g. *M. edulis* (Malone and Dodd, 1967)). A specific osmoregulation is probably

375 not needed for CWC in the mostly salinity stable habitats they live in (Roberts et al., 2009).

376 Reduced growth rates consequently lower the amount of lattice defects and the amount of

377 possible incorporation sites for sodium (Mucci, 1988; White, 1977; Yoshimura et al., 2017), if

378 bulk extension-rates are indeed related to crystal growth rates.

379 If Na/Ca ratios in corals are controlled by calcification rates, a calcification rate proxy could be

380 used to correct this effect. Sr/Ca ratios have been discussed as a possible growth rate proxy

381 (de Villiers et al., 1994) and may be used to determine changes in growth rate. However, our

382 data shows that the Sr/Ca ratios remain constant with changing salinities. Accordingly,

383 concluding from the results of de Villiers et al. (1994) the calcification rate would remain

384 constant over the whole salinity range. It should be noted that higher growth rates do not

385 necessarily imply higher calcification rates or vice versa. Higher growth rate can also be

386 caused by higher organic deposits in the skeleton (Stolarski, 2003). Therefore, a change in

387 calcification cannot necessary be inferred from changing Sr/Ca ratios. Still, the effects that

388 growth or calcification rate changes and the different skeletal architectures have on Sr/Ca

389 ratios in corals is still discussed. There is evidence for positive and negative correlation of

390 Sr/Ca with growth and calcification rate as well as the different skeletal architectures (Allison

391 and Finch, 2004; Cohen et al., 2006; Kunioka et al., 2006; Raddatz et al., 2013). It still remains

392 unknown why there is no persistent Sr/Ca variation between the differential skeletal

393 architectures (COC, fibrous deposits) in this study despite being visible in several other studies

394 (Cohen et al., 2006; Gagnon et al., 2007; Raddatz et al., 2013). An explanation could be the

395 low sampling resolution in the profiled samples and possible mixing of COC and fibrous zone

396 material. Further research is needed to evaluate the effects of growth and calcification rates

397 on Sr/Ca ratios in biogenic carbonates.

398 **4.2.2. Temperature**

399 A temperature control on Na/Ca ratios has been shown in inorganic precipitated aragonite

400 (White, 1977) and in the planktonic foraminifera *G. ruber* and *G. sacculifer* (Mezger et al.,

401 2016), although temperature and salinity covary in that study. Furthermore, Rollion-Bard and

402 Blamart (2015) suggest a possible temperature control on Na/Ca ratios in the CWC *D.*

403 *pertusum* and the warm-water coral *Porites* sp. However, the temperature sensitivity in

404 inorganically precipitated aragonite is far lower compared to the biogenic aragonite from CWC

405 including a systematic offset of $K_d^{Na}{}_{(15°C)}$= 1.17*10^{-4}. Interestingly, other marine carbonates

406 (*Porites* sp., *M. edulis*) also fit in the calculated temperature sensitivity. This holds true for

407 biogenic aragonite and biogenic calcite, where *M. edulis* fits into the temperature sensitivity

408 found by Mezger et al. (2016). A combined regression using the data from Evans et al. (2018),

409 Mezger et al. (2016) and Lorens and Bender (1980) reveals a temperature sensitivity of -0.37

410 mmol/mol/°C which is strikingly similar to the sensitivity in aragonite of -0.31 mmol/mol/°C (Fig.

411 6). The samples that Mezger et al. (2016) used in their study derive from the Red Sea, where

412 a negative correlation between the seawater salinity and seawater temperature exists. They

413 conclude that the salinity effect on Na/Ca ratios and the covariance between salinity and

414 temperature cause the temperature sensitivity of Na/Ca ratios. However, it is also possible that

415 the salinity sensitivity is caused by a temperature effect.

416 The apparent offset between inorganically precipitated aragonite and biogenic carbonates

417 further implies a biological control on Na incorporation. In contrast to other elements such as

418 Lithium (Montagna et al., 2014), the high correlation between *D. pertusum, M. oculata*,

419 Caryophylliidae, *Porites* sp. and *M. edulis* implies that the Na/Ca variance introduced by these

420 possibly occurring vital effects appear to be similar for all these species. We suggest that

similar Na pathways into the calcifying space exist in foraminifera, mussels and scleractinian warm-water as well as cold-water corals and temperature exerts a strong control on the activity of these pathways, altering the sodium availability during calcification. Further controls are possibly contributed by temperature dependent solubility variations of $CaCO_3$ and Na_2CO_3 and an exothermic Na incorporation mechanism.

Bertlich et al. (2018) proposed that lower temperatures increase the solubility of calcium carbonate and increase the amount of free Ca, leading to higher Na/Ca ratios at lower temperatures. Yet such a solubility-controlled temperature effect on calcite and aragonite is rather small, whereas the sensitivity to pressure changes is much more pronounced (Pytkowicz and Conners, 1964; Zeebe and Wolf-Gladrow, 2001). Accordingly, the Na/Ca ratio should also decrease with water depth. Here we do observe a relationship between Na/Ca ratios and water depth, but at constant temperatures (7.2°C – 7.8°C) there is no effect of water depth (160 m – 280 m) on Na/Ca ratios. The relationship between depth and Na/Ca ratios is therefore presumably caused by the positive correlation between water temperature and water depth. A decrease in Na/Ca ratios with temperatures could also be explained by solubility effects similar to the effects that are discussed to cause the temperature effects on Li/Ca ratios (Marriott et al., 2004). The solubility of Na_2CO_3 increases with increasing temperature (Haynes et al., 2016). Again, this would result in decreasing Na/Ca ratios with increasing temperature, because the solubility of Na_2CO_3 decreases relative to calcium carbonate (Haynes et al., 2016), making it thermodynamically less favorable to incorporate Na. The effects of pressure on the solubility of Na_2CO_3 cannot be quantified at the moment due to the lack of studies.

Moreover, the temperature effect can also be caused by an exothermic substitution mechanism of Na into the aragonite lattice, similar to the incorporation of Mg in calcite (Mucci and Morse, 1990). If the substitution between Ca and Na is exothermic, consequently the incorporation of Na is favored at lower temperatures. However, there is to our knowledge, no study available that contains enthalpy data for this reaction. While the proposed mechanism by Bertlich et al., (2018) can be excluded as an explanation for the temperature sensitivity of

448 Na/Ca ratios, the other explanations are equally plausible in terms of the existing studies. Still,

449 the differences in the temperature sensitivity between inorganic precipitated aragonite and

450 biogenic aragonite requires further biological controls to explain this deviation.

451 As an alternative, we explore whether temperature dependent Na membrane pathways can

452 explain temperature effects on aragonitic Na/Ca ratios. There are several enzymes and ion

453 pumps known that constitute sodium pathways through the membrane of the calcifying space.

454 Na^+/K^+-ATPase are known from the tropical coral *Galaxea fascicularis* (Ip and Lim, 1991),

455 Na/Ca ion pumps are suggested to exist in *Galaxea fascicularis* and *Tubastraea faulkneri*

456 (Marshall, 1996)*.* Na^+/K^+-ATPase was found in the bivalve species *M. edulis* and *Limecola*

457 *balthica* (Pagliarani et al., 2006; Wang and Fisher, 1999) as well as Na/Mg ion pumps in

458 *Ruditapes philippinarum* and *Mytilus galloprovincialis* (Pagliarani et al., 2006). Whether these

459 enzymes exist in *D. pertusum* is unknown, but since corals possess a nervous system (Chen

460 et al., 2008) and *D. pertusum* shows reaction to electrical stimulation (Shelton, 1980) at least

461 the existence of Na^+/K^+-ATPase must be assumed. However, it remains unclear if this enzyme

462 participates in the modification of the calcifying fluid. The participation of Na/Ca ion pumps is

463 also plausible, since it would result in higher Ca-concentrations in the calcifying space which

464 would aid the calcification process due to the high transport capacity (Carafoli et al., 2001).

465 Membrane calcium pumps on the other hand are better suited to transport Ca from a

466 compartment with low Ca-concentrations, which is not applicable when considering seawater

467 as the source compartment (Wang et al., 1992). Since the activity of enzymes is a function of

468 temperature (Sizer, 2006), a temperature control of the ion concentration in the calcifying fluid

469 has to be considered. Rising temperatures would increase the activity of the particular enzyme

470 following the Arrhenius equation (Arrhenius, 1896) and consequently lower the Na-

471 concentration in the calcifying space. Unfortunately, it is impossible to quantify these effects

472 from the data at hand, because the optimum temperature and activation energy is not enzyme

473 specific, but further controlled by enzyme and substrate purity and the presence of inhibitors

474 or activators. Specific research is needed to identify the particular enzyme in these corals as

475 well as determine the rate of ion-exchange, although we note that an enzymatic control on

476 aragonitic Na/Ca ratios does not necessarily imply a temperature control. In addition, besides

477 a temperature control, there is also a pH control on enzyme activity (Trivedi and Danforth,

478 1966). While a positive correlation between Na/Ca and seawater pH is present in the samples

479 utilized here, it is not possible to determine if this is caused by pH-controlled enzymatic activity

480 or due to an increased calcification rate. Higher seawater pH would cause higher calcification

481 fluid pH which would consequently also increase the aragonite saturation in the calcifying fluid

482 (McCulloch et al., 2012). The degree of pH elevation in the coral calcifying space would

483 therefore decrease, ultimately conserving energy ($\approx$ 10 % / -0.1 pH_{SW}) which can be used for

484 ATP-dependent transport proteins, pumping more Ca or CO_3^{2-}, leading to faster calcification

485 (McCulloch et al., 2012). It is also possible that the apparent sensitivity of Na/Ca to pH changes

486 is caused by the negative covariance of pH and temperature

487 Admittedly, the above discussion is only viable under the assumption of a closed calcifying

488 space with a much lower $[Na]_{ECF}$ than $[Na]_{Seawater}$. In the case of an open or semi-enclosed

489 calcifying space with $[Na]_{ECF}$ close or equal to $[Na]_{Seawater}$ the amount of Na removed by

490 enzymes or other ion-pumps is far too low to cause any significant changes in the composition

491 of the calcifying fluid with regards to Na. In combination with the low distribution coefficient,

492 changes in the Na-concentration of the ECF cannot cause the high variability of the skeletal

493 Na/Ca ratios. Since there is evidence for an at least semi-enclosed calcifying space (Tambutté

494 et al., 2011) we also consider this option. As described in Sec. 3.3 it is possible to calculate

495 the Mg-concentration of the ECF under the assumption of seawater leakage into the calcifying

496 space (Adkins et al., 2003; Gagnon et al., 2012) and a resulting approximately constant Na-

497 concentration. Based on this hypothesis, and the calculations defined in Eq. 3 and 4, we show

498 that the Mg-concentration in the ECF is constant, but with changing Ca-concentration (Fig. 7).

499 There is a large degree of scatter in the $[Mg]_{ECF}$ reconstructions (Fig. 7), which we suggest is

500 unlikely to represent real changes in the ECF [Mg] as it is difficult to envisage a purpose for

501 elevating $[Mg]_{ECF}$ above the of seawater given that it plays an inhibitory role in calcium

502 carbonate precipitation by acting antagonistic to the calcium transport (Okazaki, 1956; Swart,

503 1981; Yamazato, 1966). It may be that the scatter above seawater values is derived from the

504   presence of organic material, as a small positive bias in measured coral Mg/Ca would result in

505   a large overestimation of $[Mg]_{ECF}$. Crucially however, we find that $[Mg]_{ECF}$ does not change as

506   a function of $[Ca]_{ECF}$, with the implication that in this model changing skeletal Mg/Ca and Na/Ca

507   ratios are not caused by changes of the Mg or Na-concentration of the ECF but rather are

508   entirely explicable through changes in the Ca-concentration. Again, this might be caused by

509   temperature-dependent enzyme or ion-pump activity. Higher temperatures would then cause

510   a higher exchange capacity (Elias et al., 2001), leading to higher Ca- (Fig. 7) and marginally

511   lower Na-concentrations in the ECF and consequently lower Mg/Ca and Na/Ca ratios. An

512   elevation of [Ca] in the ECF and the calcifying front is also supported by recent studies from

513   Decarlo et al., (2018) and Sevilgen et al., (2019), who conducted Raman spectroscopic, $\delta^{11}B$

514   and microsensor measurements on *Pocillopora damicornis, Acropora youngei* and *Stylophora*

515   *pistilla*. The results furthermore indicate the involvement of transcellular pathways to elevate

516   the Ca-concentration in the ECF (Sevilgen et al., 2019).

517   Even though a clear correlation between temperature and Na/Ca is present, the usefulness of

518   Na/Ca ratios is greatly reduced due to the large intraspecies variability. At 6°C Na/Ca ratios

519   vary by up to 20% and even up to 10 % in a single polyp. There are several possible reasons

520   for this variability. One is the insufficient removal of the COC during the sampling process. Due

521   to the high growth rate and high organic content in the COC, elements, such as Mg, Na and Li

522   are enriched whereas other like U are depleted (Gagnon et al., 2007; Raddatz et al., 2013,

523   2014b; Robinson et al., 2014; Rollion-Bard and Blamart, 2014, 2015). This effect would also

524   explain the high Na/Ca values in corals from the Mediterranean Sea (T=13.56°C). It is possible

525   that during the sampling process a larger amount of the fibrous deposits was removed in

526   comparison to the other samples. This would cause a greater effect of the enriched COC

527   material and therefore cause higher Na/Ca ratios. It is therefore preferable to use in-situ

528   techniques (laser ablation, EPMA, SIMS) instead of solution-based chemistry and profile

529   measurements through the theca wall instead of bulk samples, because it allows for a better

530   recognition and removal of values that derive from COC or COC-like structures. Seasonality

531   could be also a factor responsible for a percentage of the variation, but the sampled corals

originate from depths where seasonality presumably only plays a minor role. An estimated seasonal temperature change of 4°C only suffices to explain 1 mmol/mol variation but not the observed variation of 10 mmol/mol. From this, it can be inferred that there must be other controls on Na/Ca ratios besides water temperature. Diurnal temperature fluctuations caused by internal waves as found for example in the Rockall Trough are also not high enough (3°C) to explain these variations (Mienis et al., 2007). As mentioned in Sec 4.1, calcification rates constitute a major control on Na/Ca ratios by controlling the amount of incorporation sites for Na (Kitano et al., 1975; Mucci, 1988; White, 1977; Yoshimura et al., 2017). Therefore, numerous second order control factors could cause variations in the Na/Ca ratios by controlling the calcification rate. These second order controls include nutrient availability and supply, changes in the carbonate system, coral fitness and many more. Some of these controls (nutrient supply, coral fitness) have the potential to vary with a high spatial resolution and consequently cause great variations in Na/Ca ratios even if the samples derive from the same colony.

4.3. Na/Mg ratios to overcome vital effects

Even though a good correlation of R^2=0.9 between Na/Ca and temperature is observable in our data, the samples from the Mediterranean Sea (T=13.54°C) show slightly elevated Na/Ca ratios. Reasons for this are discussed in Sec. 4.2. Rollion-Bard and Blamart (2015) proposed Na/Mg ratios to overcome these effects. The basis for this is that Na/Ca and Mg/Ca ratios could be controlled by similar vital effects such as growth rate and the amount of organic content. Combining Na/Ca and Mg/Ca ratios reduces the impact of these effects, though the temperature sensitivity of Na/Ca ratios is preserved as Mg/Ca ratios show no apparent correlation with temperature (Fig. 8). The resulting regression between Na/Mg and temperature yields the following equation:

$$f_{T\,6-22°C} = 7.1 \pm 0.17 - 0.07 \pm 0.01 \times T \ (R^2 = 0.92, P = 0.009) \tag{5}$$

The application of Na/Mg in this study does not significantly improve the regression, as it removes the inverse correlation between 6 and 10°C. This might be caused by covariance

559   between sodium and magnesium. It was shown that magnesium in the parent solution reduces

560   the amount of incorporated sodium (Okumura and Kitano, 1986). However, utilizing Na/Mg

561   ratios removes the striking irregularity at 13.54 °C. The large scatter, however, is not

562   significantly reduced which implies further vital effects that cannot be resolved with this

563   technique. To overcome this the mean of at least 10 analyzed samples should be used to

564   obtain reliable results. If these prerequisites are fulfilled, Na/Mg and Na/Ca could provide a

565   means of reconstructing temperature. This could prove useful especially for temperature

566   reconstructions in deep time on organisms that are extinct today. In this case the nearest living

567   relative principle is used, which potentially introduces large errors. Further research on

568   different aragonitic and calcitic organisms is necessary to detect further species that show the

569   same temperature sensitivity. If it is shown that Na/Ca and/or Na/Mg ratios show no species-

570   specific variations, empirical calibrations could be applied to extinct species for which proxy

571   calibrations are not possible. Still though, when using Na/Ca for temperature reconstructions

572   changes in seawater have to be considered that would lead to an underestimation of

573   temperature at high pH. However, Na/Mg show no sensitivity to changes in seawater pH, so

574   by combining Na/Ca and Mg/Ca ratios this effect can be ignored.

575   **5. Conclusion**

576   The data at hand does not support the utility of Na/Ca in cold-water corals as a salinity proxy

577   as proposed by Wit et al., (2013) and Mezger et al., (2016) for biogenic calcite. While there is

578   a positive trend between Na/Ca and salinity when excluding data from the Red Sea samples,

579   it is not statistically significant.

580   A significant inverse correlation between temperature and Na/Ca ratios is present, which

581   cannot be explained by a co-variance of temperature and salinity (c.f. Mezger et al., 2016).

582   Two additional organisms, *Porites* sp. (Mitsuguchi et al., 2001; Ramos et al., 2004) and *M.*

583   *edulis* (Lorens and Bender, 1980) fit in this regression too. The mechanism of sodium

584   incorporation therefore appears to be consistent between these three species. We propose

585   temperature-dependent activity in Na-ion or Ca-ion transport proteins as the underlying

mechanism behind the observable correlation. While the intraspecies and intraindividual variation is large, Na/Ca can be well correlated to environmental variables when based on the averages of several specimens. Therefore, Na/Ca ratios might provide a temperature-proxy that is usable for a wide variety of aragonitic organisms and maybe even calcitic organisms. As proposed by Rollion-Bard and Blamart (2015), Na/Mg ratios can be used to correct for inconsistencies during the sampling process.

Author contribution

Jacek Raddatz and Nicolai Schleinkofer designed the experiments and conducted the measurements. Jacek Raddatz, Andre Freiwald, Lydia Beuck, Andres Rüggeberg and Volker Liebetrau provided samples and environmental data. Nicolai Schleinkofer prepared the manuscript with contributions from all co-authors.

Acknowledgements

We are grateful to all cruise captains, crew members and cruise participants of research cruises POS325, POS391, POS455, POS 385, M61, POS625, B10-17a/b, 64PE284, M70/1, COR2, MSM20-4, KRSE2013 and RV Gunnerus. Ship time of RV Belgica was provided by BELSPO and RBINS–OD Nature. Cruise POS391 was realized by DFG Project RI 598/4-1. JR acknowledges funding from DFG project ECHO RA 2516-1. AR acknowledges support from Swiss National Science Foundation, SNF project number 200021_149247.

FIERCE is financially supported by the Wilhelm and Else Heraeus Foundation, which is gratefully acknowledged. This is FIERCE contribution No. 002

611

612

613

614

615

616

617

618

619

620

621

622

623

624

625

626

627

628

629

630

631

632

633

634

635

636

637

638

639

640

641

642 **Figures**

643
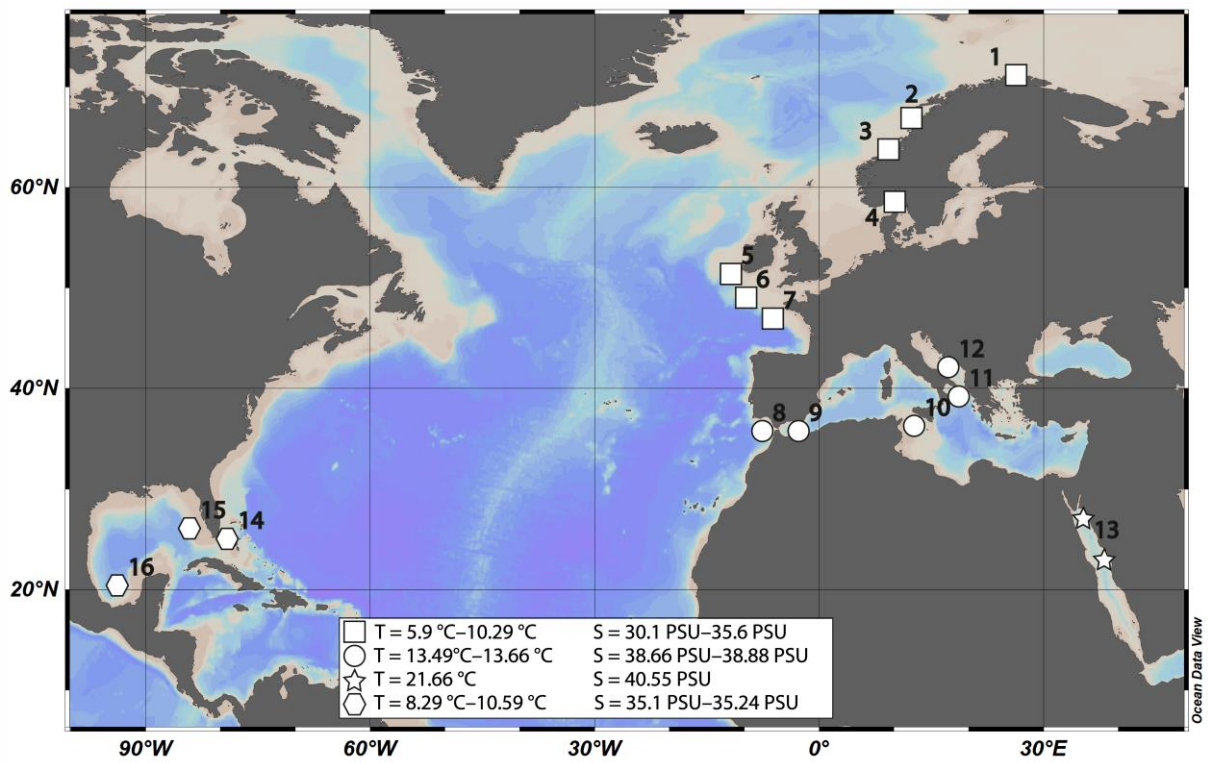
Figure 1 Map of sampling locations. Locations are grouped in four areas with similar physical parameters. 1: Lopphavet, Sotbakken, Stjernsund; 2: Traenadjupet; 3: Sula, Nordleksa, Tautra, Røberg; 4: Oslofjord; 5: Galway Mound, 6: Whittard Canyon; 7: Guilvinec Canyon; 8: Meknes Carbonate Mound Province 9: El Idrissi Bank; 10: Urania Bank; 11: Santa Maria di Leuca (SML) Province, 12: Bari Canyon; 13: Red Sea; 14: Great Bahama Bank; 15: Southwest Florida; 16: Campeche Bank

649

650
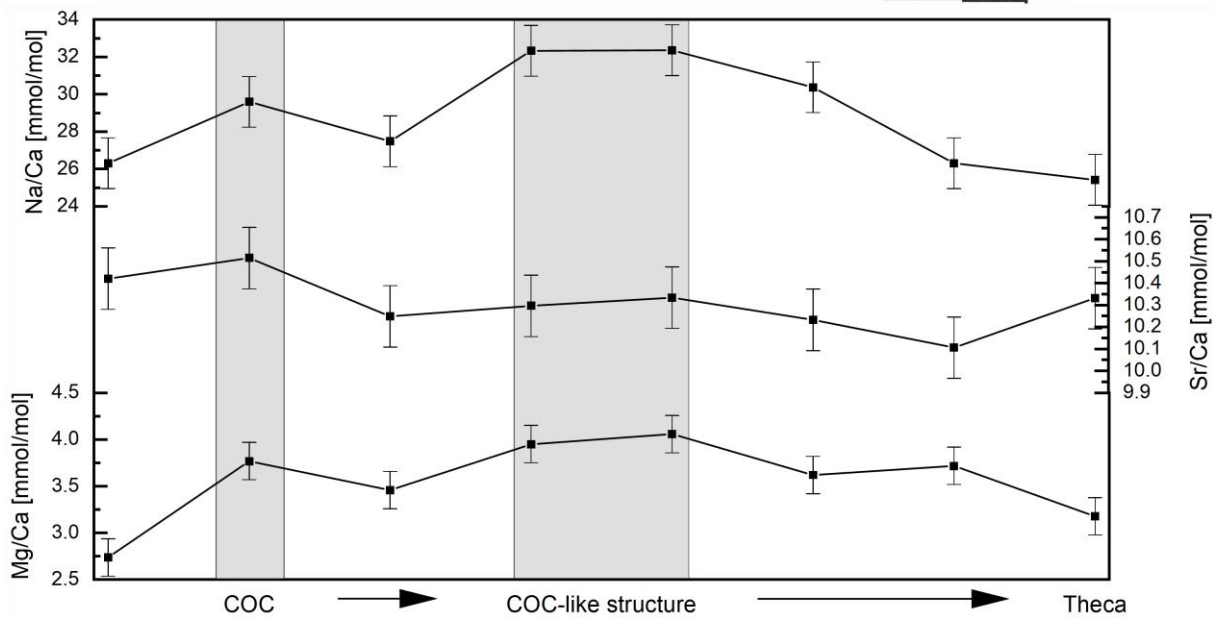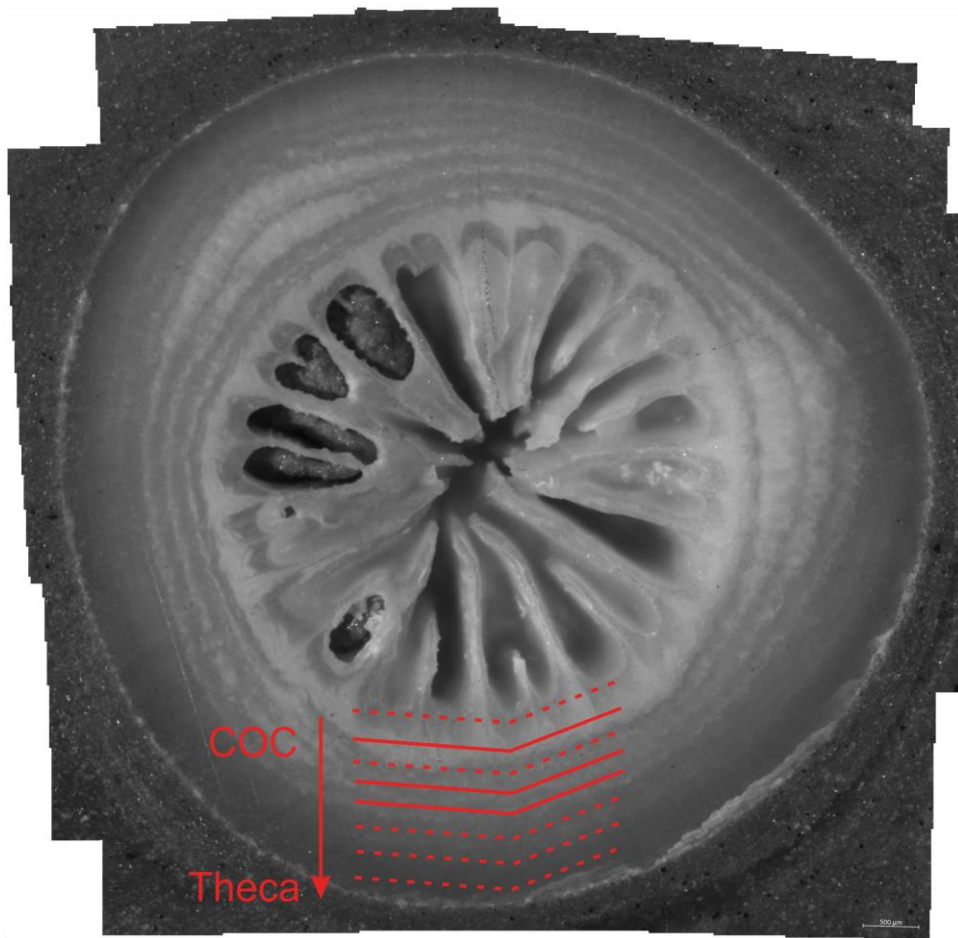
Figure 2 Intra-individual element heterogeneities of one sample from Lopphavet (*D. pertusum*). Shaded-grey areas indicate COC and COC-like structures (solid lines in sample picture). Error bars indicate 2SD of the JCp-1 mean. Within the uncertainty Sr/Ca ratios show no significant changes throughout the coral, whereas Mg/Ca and Na/Ca show variations of 1.25 mmol/mol and 6 mmol/mol respectively.

651
652
653
654

655
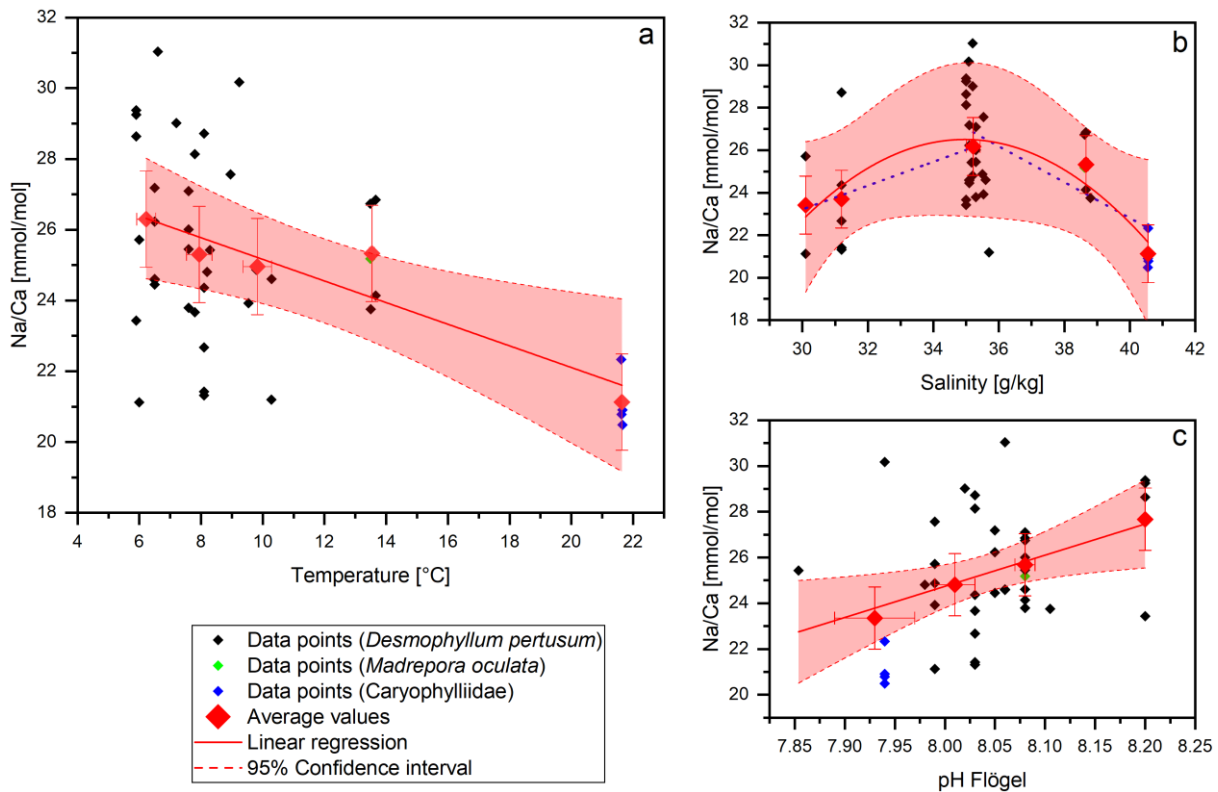
Figure 3 Na/Ca Data (without COC) plotted against water temperature, salinity and pH. Red diamonds
indicate averaged values for temperature ranges. Temperature ranges are 5–7°C, 7–9°C, 9–11°C, 13–15°C
and 21–23°C. X-Error relates to the SD of the temperature/salinity mean. Y- Error bars indicate 2SD of the
JCp-1 mean. Red lines are linear regressions of the averaged values with the 95 % confidence interval
shaded. Blue dotted lines indicate linear regressions for different salinity ranges.

661
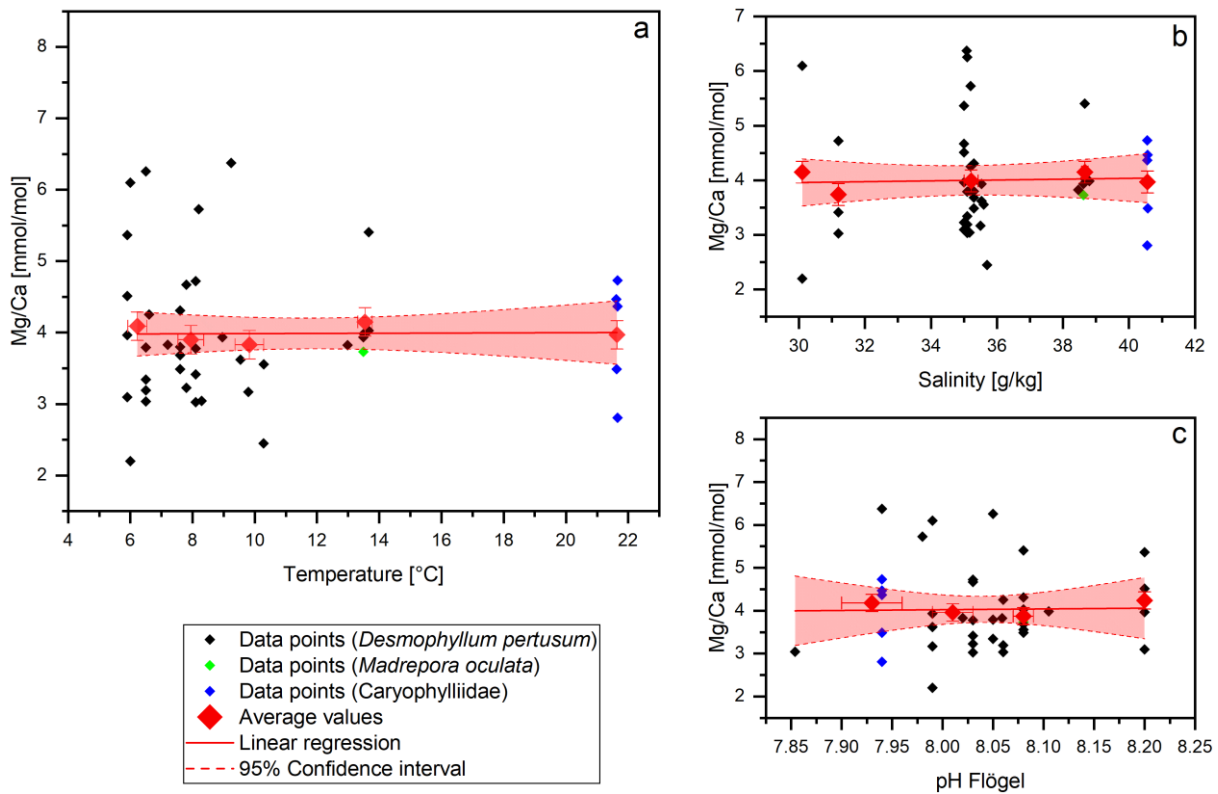
Figure 4 Mg/Ca Data (without COC) plotted against water temperature, salinity and pH. Red diamonds
indicate averaged values for temperature ranges. Temperature ranges are 5–7°C, 7–9°C, 9–11°C, 13–15°C
and 21–23°C. X-Error relates to the SD of the temperature/salinity mean Y- Error bars indicate 2SD of the

JCp-1 mean. Red lines are linear regressions of the averaged values with the 95 % confidence interval shaded.
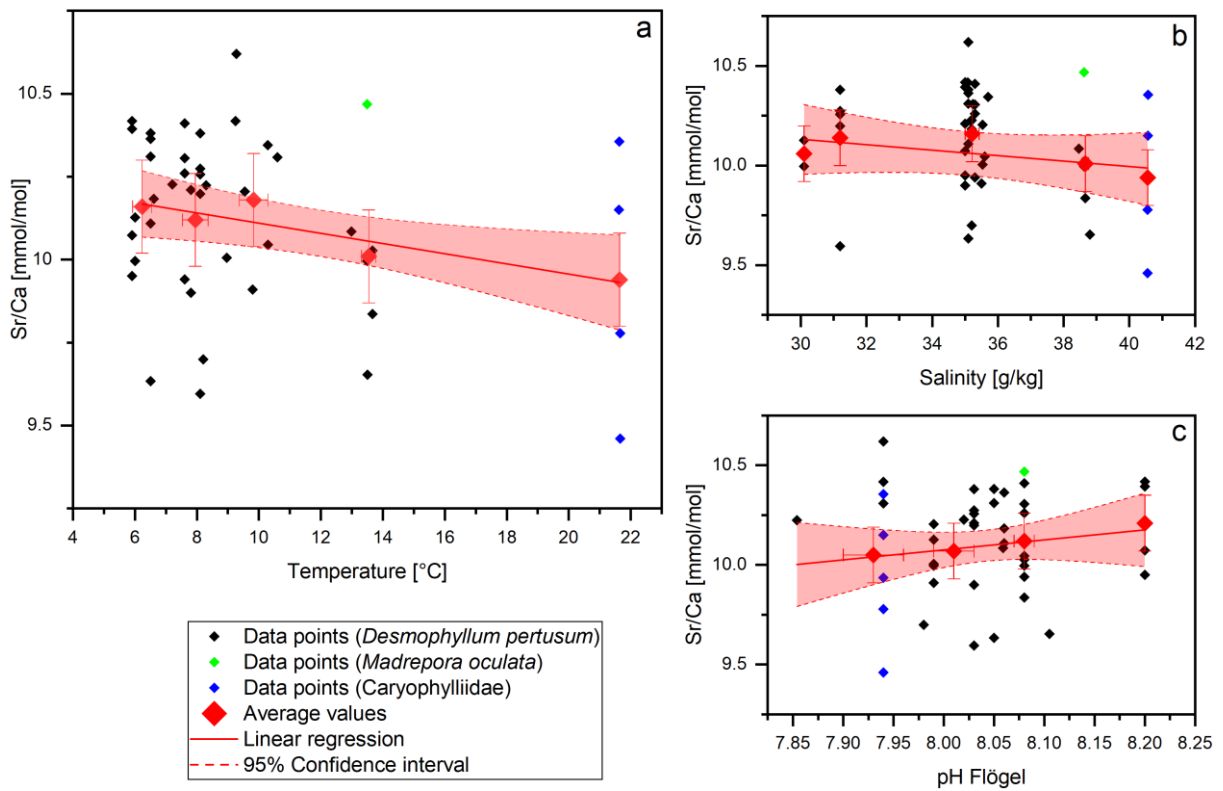
Figure 5 Sr/Ca Data (without COC) plotted against water temperature, salinity and pH. Red diamonds indicate averaged values for temperature ranges. Temperature ranges are 5–7°C, 7–9°C, 9–11°C, 13–15°C and 21–23°C. X-Error relates to the SD of the temperature/salinity mean. Y- Error bars indicate 2SD of the JCp-1 mean. Red lines are linear regressions of the averaged values with the 95 % confidence interval shaded.
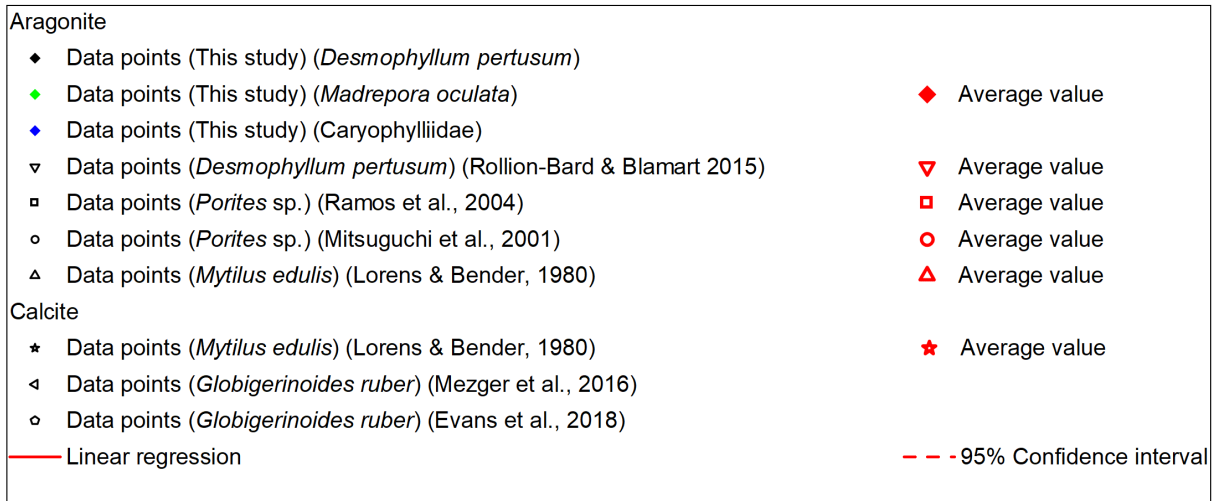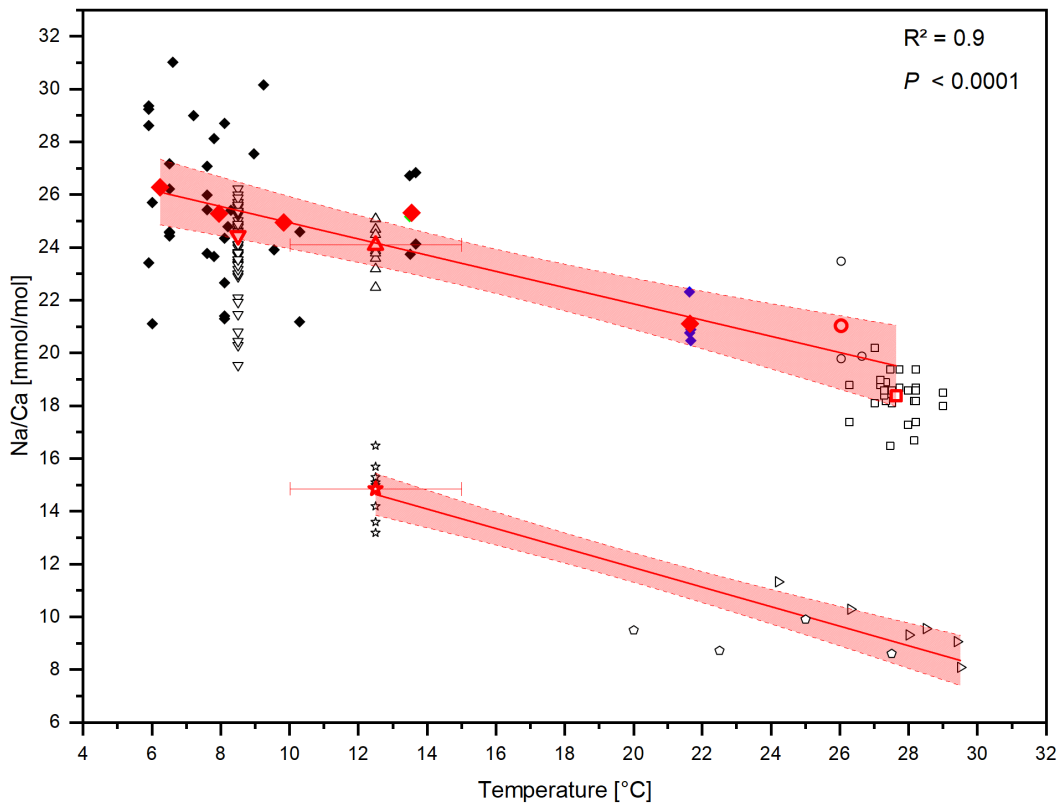
Figure 6 Compiled Na/Ca ratios from different studies. *D. pertusum, M. oculata, M. edulis* **and** *Porites* **sp. show a negative linear relation with water temperature. R² relates only to the aragonitic samples Calcitic samples from** *M. edulis* **and** *Globigerinoides ruber* **show the same sensitivity, albeit with an offset of 10 mmol/mol. Temperature for the data from Lorens & Bender amounts to the average temperature of the tank the corals were cultivated in while the error bars show maximum and minimum values.**

682
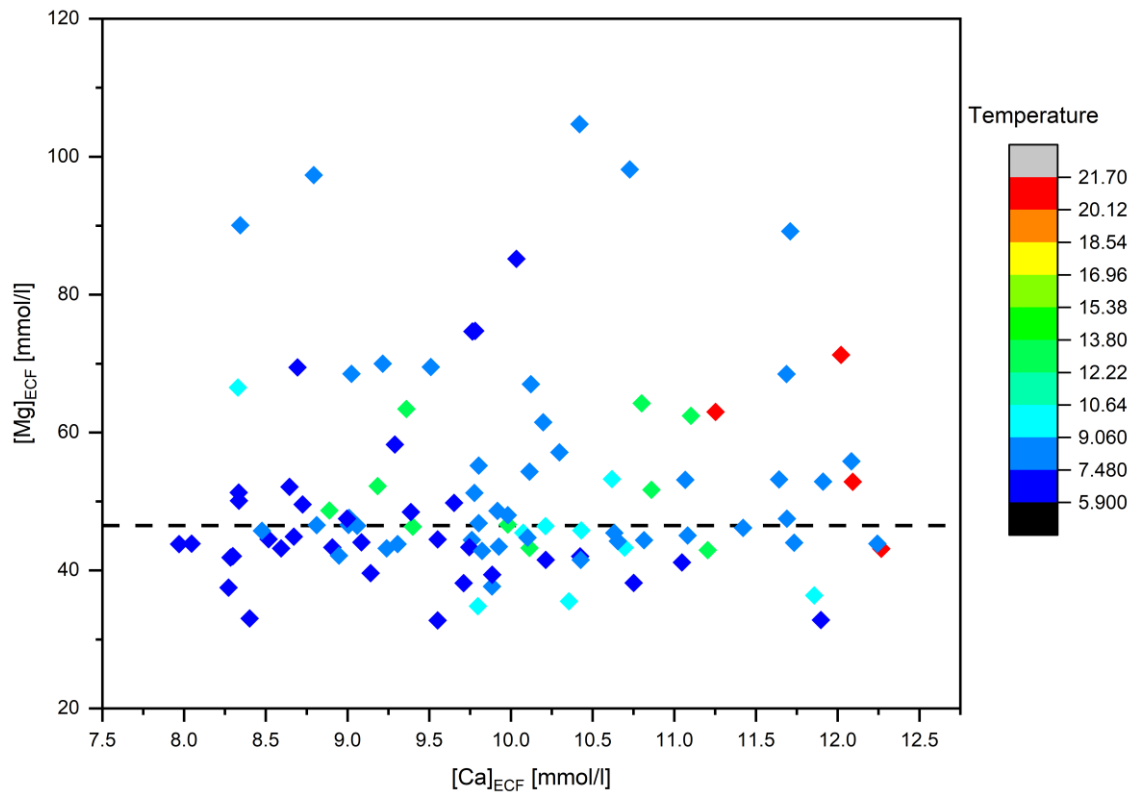
Figure 7 Calcium and Magnesium concentration in the ECF of the investigated corals. The color of the data points indicate the ambient water temperature, which is increasing with increasing Ca-concentrations. The dashed line indicates the median of the Mg-concentration in the ECF.

686
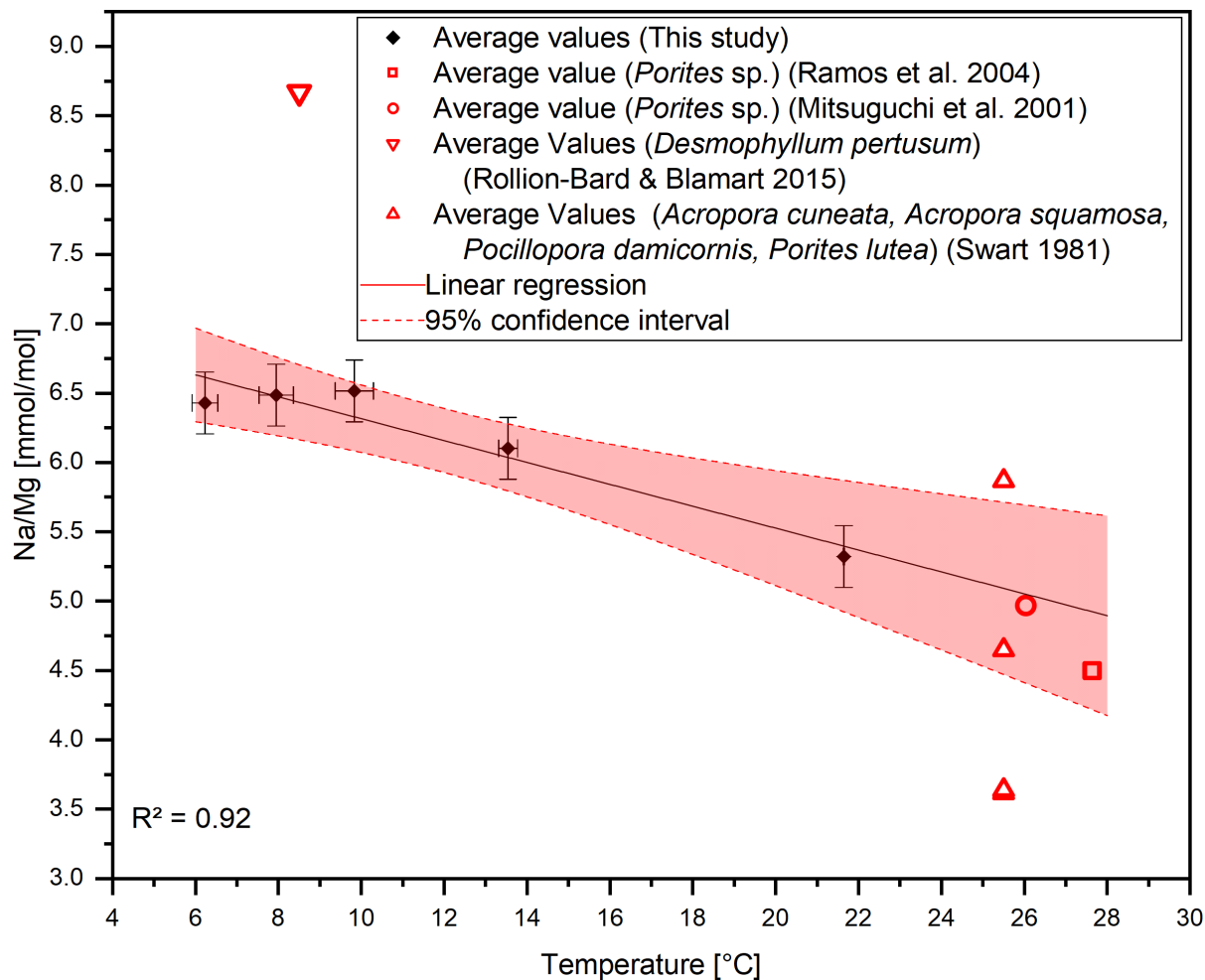
Figure 8 Na/Mg ratios from this study vs. water temperature. Na/Mg ratios can be used to correct for the sampling of varying proportions of different domains. Y-Error bars relate to 2SD of the JCp-1 measurements. X-Error bars relate to 1SD of the temperature mean for the chosen temperature ranges.

687
688
689

690

691

692

693

694

695

696

697

698

699

700

701

702

 Tables

	Na/Ca			Sr/Ca			Mg/Ca		
Temperature [°C]	mmol/mol	n	SD	mmol/mol	n	SD	mmol/mol	n	SD
6.23 ± 0.31	26.30	12	2.88	10.16	12	0.23	4.09	12	1.27
7.94 ± 0.41	25.30	15	2.48	10.13	15	0.24	3.90	14	0.74
9.83 ± 0.46	24.96	5	3.26	10.18	5	0.21	3.83	5	1.49
13.56 ± 0.09	25.33	5	1.43	10.01	6	0.27	4.15	6	0.62
21.64 ± 0.02	21.13	4	0.82	9.94	5	0.34	3.97	5	0.8
	Na/Ca			Sr/Ca			Mg/Ca		
Average Salinity [g/kg]	mmol/mol	n	SD	mmol/mol	n	SD	mmol/mol	n	SD
30.1	23.42	2	2.25	10.06	2	0.09	4.15	2	2.75
31.2	23.70	5	3.06	10.14	5	0.31	3.74	4	0.73
35.22 ± 0.21	26.18	25	2.46	10.16	25	0.22	3.99	25	1.01
38.67 ± 0.07	25.33	5	1.43	10.01	6	0.27	4.16	6	0.62
40.56 ± 0.01	21.13	4	0.82	9.94	5	0.34	3.97	5	0.8

705 **Table 1 Na/Ca, Sr/Ca, Mg/Ca mean values measured with ICP-OES, standard deviation and sample number.**
706 **Values relate to certain salinity and temperature envelopes.**

707

708

709

710

711

712

713

714

715

716

717

718

719

720

References

Adkins, J. F., Boyle, E. A., Curry, W. B. and Lutringer, A.: Stable isotopes in deep-sea corals and a new mechanism for "vital effects," Geochim. Cosmochim. Acta, 67(6), 1129–1143, doi:10.1016/S0016-7037(00)01203-6, 2003.

Al-Horani, F. A., Al-Moghrabi, S. M. and De Beer, D.: The mechanism of calcification and its relation to photosynthesis and respiration in the scleractinian coral Galaxea fascicularis, Mar. Biol., 142(3), 419–426, doi:10.1007/s00227-002-0981-8, 2003.

Allemand, D., Tambutté, É., Zoccola, D. and Tambutté, S.: Coral Calcification, Cells to Reefs, in Coral Reefs: An Ecosystem in Transition, pp. 119–150, Springer Netherlands, Dordrecht., 2011.

Allen, K. A., Hönisch, B., Eggins, S. M., Haynes, L. L., Rosenthal, Y. and Yu, J.: Trace element proxies for surface ocean conditions: A synthesis of culture calibrations with planktic foraminifera, Geochim. Cosmochim. Acta, 193, 197–221, doi:10.1016/j.gca.2016.08.015, 2016.

Allison, N. and Finch, A. A.: High-resolution Sr/Ca records in modern Porites lobata corals: Effects of skeletal extension rate and architecture, Geochemistry, Geophys. Geosystems, 5(5), doi:10.1029/2004GC000696, 2004.

Amiel, A. J., Friedman, G. M. and Miller, D. S.: Distribution and nature of incorporation of trace elements in modern aragonitic corals*, Sedimentology, 20(1), 47–64, doi:10.1111/j.1365-3091.1973.tb01606.x, 1973.

Anagnostou, E., Sherrell, R. M., Gagnon, A., LaVigne, M., Field, M. P. and McDonough, W. F.: Seawater nutrient and carbonate ion concentrations recorded as P/Ca, Ba/Ca, and U/Ca in the deep-sea coral Desmophyllum dianthus, Geochim. Cosmochim. Acta, 75(9), 2529–2543, doi:10.1016/j.gca.2011.02.019, 2011.

Anagnostou, E., Huang, K. F., You, C. F., Sikes, E. L. and Sherrell, R. M.: Evaluation of boron isotope ratio as a pH proxy in the deep sea coral Desmophyllum dianthus: Evidence of physiological pH adjustment, Earth Planet. Sci. Lett., 349–350(July 2015), 251–260, doi:10.1016/j.epsl.2012.07.006, 2012.

Arrhenius, S.: XXXI. On the influence of carbonic acid in the air upon the temperature of the ground, London, Edinburgh, Dublin Philos. Mag. J. Sci., 41(251), 237–276, doi:10.1080/14786449608620846, 1896.

Bertlich, J., Nürnberg, D., Hathorne, E. C., De Nooijer, L. J., Mezger, E. M., Kienast, M., Nordhausen, S., Reichart, G. J., Schönfeld, J. and Bijma, J.: Salinity control on Na incorporation into calcite tests of the planktonic foraminifera Trilobatus sacculifer - Evidence from culture experiments and surface sediments, Biogeosciences, 15(20), 5991–6018, doi:10.5194/bg-15-5991-2018, 2018.

Bett, B. J.: UK Atlantic Margin Environmental Survey: Introduction and overview of bathyal benthic ecology, Cont. Shelf Res., 21(8–10), 917–956, doi:10.1016/S0278-4343(00)00119-9, 2001.

Blamart, D., Rollion-Bard, C., Meibom, A., Cuif, J. P., Juillet-Leclerc, A. and Dauphin, Y.: Correlation of boron isotopic composition with ultrastructure in the deep-sea coral Lophelia pertusa: Implications for biomineralization and paleo-pH, Geochemistry, Geophys. Geosystems, 8(12), 1–11, doi:10.1029/2007GC001686, 2007.

Bollmann, J., Herrle, J. O., Cortés, M. Y. and Fielding, S. R.: The effect of sea water salinity on the morphology of Emiliania huxleyi in plankton and sediment samples, Earth Planet. Sci. Lett., 284(3–4), 320–328, doi:10.1016/j.epsl.2009.05.003, 2009.

Brahmi, C., Kopp, C., Domart-Coulon, I., Stolarski, J. and Meibom, A.: Skeletal growth dynamics linked to trace-element composition in the scleractinian coral Pocillopora damicornis, Geochim. Cosmochim. Acta, 99, 146–158, doi:10.1016/j.gca.2012.09.031, 2012.

Branson, O., Bonnin, E. A., Perea, D. E., Spero, H. J., Zhu, Z., Winters, M., Hönisch, B., Russell, A. D., Fehrenbacher, J. S. and Gagnon, A. C.: Nanometer-Scale Chemistry of a Calcite Biomineralization Template: Implications for Skeletal Composition and Nucleation, Proc. Natl. Acad. Sci., 113(46), 12934–12939, doi:10.1073/pnas.1522864113, 2016.

Büscher, J. V., Form, A. U. and Riebesell, U.: Interactive Effects of Ocean Acidification and Warming on Growth, Fitness and Survival of the Cold-Water Coral Lophelia pertusa under Different Food Availabilities, Front. Mar. Sci., 4(April), 1–14, doi:10.3389/fmars.2017.00101, 2017.

Busenberg, E. and Niel Plummer, L.: Kinetic and thermodynamic factors controlling the distribution of SO_3^{2-} and Na^+ in calcites and selected aragonites, Geochim. Cosmochim. Acta, 49(3), 713–725, doi:10.1016/0016-7037(85)90166-8, 1985.

Carafoli, E., Santella, L., Branca, D. and Brini, M.: Generation, control, and processing of cellular calcium signals, Crit. Rev. Biochem. Mol. Biol., 36(2), 107–260, doi:10.1080/20014091074183, 2001.

Chen, E., Stiefel, K. M., Sejnowski, T. J. and Bullock, T. H.: Model of traveling waves in a coral nerve network, J. Comp. Physiol. A Neuroethol. Sensory, Neural, Behav. Physiol., 194(2), 195–200, doi:10.1007/s00359-007-0305-z, 2008.

Chen, J.-P.: Batch and Contunuous Adsorption of Stontium by Plant Root Tissues, Bioresour. Technol., 60, 185–189, doi:10.1016/S0960-8524(97)00021-7, 1997.

Cohen, A. L., Gaetani, G. A., Lundälv, T., Corliss, B. H. and George, R. Y.: Compositional variability in a cold-water scleractinian, Lophelia pertusa: New insights into "vital effects," Geochemistry, Geophys. Geosystems, 7(12), doi:10.1029/2006GC001354, 2006.

Constantz, B. R.: Skeletal Organization in Caribbean Acropora Spp. (Lamarck), in Origin, Evolution, and Modern Aspects of Biomineralization in Plants and Animals, pp. 175–199, Springer US, Boston, MA., 1989.

Cuif, J.-P. and Dauphin, Y.: Microstructural and physico-chemical characterization of ' centers of calcification ' in septa of some Recent scleractinian corals, Paläontologische Zeitschrift, 72(November), 257–270, doi:10.1007/BF02988357, 1998.

Cuif, J. P., Dauphin, Y. Y., Doucet, J., Salome, M. and Susini, J.: XANES mapping of organic sulfate in three scleractinian coral skeletons, Geochim. Cosmochim. Acta, 67(1), 75–83, doi:10.1016/S0016-7037(02)01041-4, 2003.

Decarlo, T. M., Comeau, S., Cornwall, C. E. and McCulloch, M. T.: Coral resistance to ocean acidification linked to increased calcium at the site of calcification, Proc. R. Soc. B Biol. Sci., 285(1878), doi:10.1098/rspb.2018.0564, 2018.

Druffel, E. R. M.: Geochemistry of corals: Proxies of past ocean chemistry, ocean circulation, and climate, Proc. Natl. Acad. Sci., 94(16), 8354–8361, doi:10.1073/pnas.94.16.8354, 1997.

Dullo, W. C., Flögel, S. and Rüggeberg, A.: Cold-water coral growth in relation to the hydrography of the Celtic and Nordic European continental margin, Mar. Ecol. Prog. Ser., 371, 165–176, doi:10.3354/meps07623, 2008.

Elderfield, H. and Ganssen, G.: Past temperature and $\delta^{18}O$ of surface ocean waters inferred from foraminiferal Mg/Ca ratios, Nature, 405(6785), 442–445, doi:10.1038/35013033, 2000.

Elderfield, H., Ferretti, P., Greaves, M., Crowhurst, S. J., McCave, I. N., Hodell, D. a and Piotrowski, A. M.: Evolution of ocean temperature, Science (80-.)., 337(August), 704–709,

813   doi:10.1594/PANGAEA.786205, 2012.

814   Elias, C. L., Xue, X. H., Marshall, C. R., Omelchenko, A., Hryshko, L. V. and Tibbits, G. F.:
815   Temperature dependence of cloned mammalian and salmonid cardiac Na(+)/Ca(2+)
816   exchanger isoforms., Am. J. Physiol. Cell Physiol., 281(3), C993–C1000, doi:10.1111/j.1432-
817   1033.1984.tb08031.x, 2001.

818   Von Euw, S., Zhang, Q., Manichev, V., Murali, N., Gross, J., Feldman, L. C., Gustafsson, T.,
819   Flach, C., Mendelsohn, R. and Falkowski, P. G.: Biological control of aragonite formation in
820   stony corals, Science (80-.)., 356(6341), 933–938, doi:10.1126/science.aam6371, 2017.

821   Evans, D., Müller, W. and Erez, J.: Assessing foraminifera biomineralisation models through
822   trace element data of cultures under variable seawater chemistry, Geochim. Cosmochim.
823   Acta, 236, 198–217, doi:10.1016/j.gca.2018.02.048, 2018.

824   Evans, D., Webb, P., Penkman, K. E. H., Kroger, R. and Allison, N.: The characteristics and
825   biological relevance of inorganic amorphous calcium carbonate (ACC) precipitated from
826   seawater, Cryst. Growth Des., doi:10.1021/acs.cgd.9b00003, 2019.

827   Finch, A. A. and Allison, N.: Mg structural state in coral aragonite and implications for the
828   paleoenvironmental proxy, Geophys. Res. Lett., 35(8), 1–5, doi:10.1029/2008GL033543,
829   2008.

830   Flögel, S., Dullo, W. C., Pfannkuche, O., Kiriakoulakis, K. and Rüggeberg, A.: Geochemical
831   and physical constraints for the occurrence of living cold-water corals, Deep. Res. Part II
832   Top. Stud. Oceanogr., 99, 19–26, doi:10.1016/j.dsr2.2013.06.006, 2014.

833   Form, A. U. and Riebesell, U.: Acclimation to ocean acidification during long-term CO2
834   exposure in the cold-water coral Lophelia pertusa, Glob. Chang. Biol., 18(3), 843–853,
835   doi:10.1111/j.1365-2486.2011.02583.x, 2012.

836   Freiwald, A.: Reef-Forming Cold-Water Corals, in Ocean Margin Systems, pp. 365–385,
837   Springer Berlin Heidelberg, Berlin, Heidelberg., 2002.

838   Freiwald, A. and Roberts, J. M., Eds.: Cold-Water Corals and Ecosystems, Springer Berlin
839   Heidelberg, Berlin, Heidelberg., 2005.

840   Freiwald, A., Beuck, L., Rüggeberg, A., Taviani, M. and Hebbeln, D.: The White Coral
841   Community in the Central Mediterranean Sea Revealed by ROV Surveys, Oceanography,
842   22(1), 58–74, doi:10.5670/oceanog.2009.06, 2009.

843   Gabitov, R. I., Gaetani, G. A., Watson, E. B., Cohen, A. L. and Ehrlich, H. L.: Experimental
844   determination of growth rate effect on U6+ and Mg2+ partitioning between aragonite and fluid
845   at elevated U6+ concentration, Geochim. Cosmochim. Acta, 72(16), 4058–4068,
846   doi:10.1016/j.gca.2008.05.047, 2008.

847   Gabitov, R. I., Schmitt, A. K., Rosner, M., McKeegan, K. D., Gaetani, G. A., Cohen, A. L.,
848   Watson, E. B. and Harrison, T. M.: In situ δ 7 Li, Li/Ca, and Mg/Ca analyses of synthetic
849   aragonites, Geochemistry, Geophys. Geosystems, 12(3), n/a-n/a,
850   doi:10.1029/2010GC003322, 2011.

851   Gagnon, A. C., Adkins, J. F., Fernandez, D. P. and Robinson, L. F.: Sr/Ca and Mg/Ca vital
852   effects correlated with skeletal architecture in a scleractinian deep-sea coral and the role of
853   Rayleigh fractionation, Earth Planet. Sci. Lett., 261(1–2), 280–295,
854   doi:10.1016/j.epsl.2007.07.013, 2007.

855   Gagnon, A. C., Adkins, J. F. and Erez, J.: Seawater transport during coral biomineralization,
856   Earth Planet. Sci. Lett., 329–330, 150–161, doi:10.1016/j.epsl.2012.03.005, 2012.

857   Gordon, C. M., Carr, R. A. and Larson, R. E.: the Influence of Environmental Factors on the
858   Sodium and Manganese Content of Barnacle Shells, Limnol. Oceanogr., 15(3), 461–466,

859   doi:10.4319/lo.1970.15.3.0461, 1970.

860   Hathorne, E. C., Gagnon, A., Felis, T., Adkins, J., Asami, R., Boer, W., Caillon, N., Case, D.,
861   Cobb, K. M., Douville, E., DeMenocal, P., Eisenhauer, A., Garbe-Schönberg, D., Geibert, W.,
862   Goldstein, S., Hughen, K., Inoue, M., Kawahata, H., Kölling, M., Cornec, F. L., Linsley, B. K.,
863   McGregor, H. V., Montagna, P., Nurhati, I. S., Quinn, T. M., Raddatz, J., Rebaubier, H.,
864   Robinson, L., Sadekov, A., Sherrell, R., Sinclair, D., Tudhope, A. W., Wei, G., Wong, H., Wu,
865   H. C. and You, C.-F.: Interlaboratory study for coral Sr/Ca and other element/Ca ratio
866   measurements, Geochemistry, Geophys. Geosystems, 14(9), 3730–3750,
867   doi:10.1002/ggge.20230, 2013.

868   Hauzer, H., Evans, D., Müller, W., Rosenthal, Y. and Erez, J.: Calibration of Na partitioning in
869   the calcitic foraminifer Operculina ammonoides under variable Ca concentration: Toward
870   reconstructing past seawater composition, Earth Planet. Sci. Lett., 497, 80–91,
871   doi:10.1016/j.epsl.2018.06.004, 2018.

872   Haynes, W. M., Lide, D. R. and Bruno, T. J.: CRC Handbook of chemistry and physics : a
873   ready-reference book of chemical and physical data., 2016.

874   Henry, L.-A. and Roberts, J. M.: Global Biodiversity in Cold-Water Coral Reef Ecosystems, in
875   Marine Animal Forests, pp. 1–21, Springer International Publishing, Cham., 2016.

876   Holcomb, M., Cohen, A. L., Gabitov, R. I. and Hutter, J. L.: Compositional and morphological
877   features of aragonite precipitated experimentally from seawater and biogenically by corals,
878   Geochim. Cosmochim. Acta, 73(14), 4166–4179, doi:10.1016/j.gca.2009.04.015, 2009.

879   Ip, Y. K. and Lim, A. L. L.: Are calcium and strontium transported by the same mechanism in
880   the hermatypic coral Galaxey fascicularis?, J. Exp. Biol., 159, 507–513, 1991.

881   Ishikawa, M. and Ichikuni, M.: Uptake of sodium and potassium by calcite, Chem. Geol.,
882   42(1–4), 137–146, doi:10.1016/0009-2541(84)90010-X, 1984.

883   Israelson, C. and Buchardt, B.: Strontium and oxygen isotopic composition of East
884   Greenland rivers and surface waters: Implication for palaeoenvironmental interpretation,
885   Palaeogeogr. Palaeoclimatol. Palaeoecol., 153(1–4), 93–104, doi:10.1016/S0031-
886   0182(99)00068-1, 1999.

887   Jurikova, H., Liebetrau, V., Raddatz, J., Fietzke, J., Trotter, J., Rocholl, A., Krause, S.,
888   McCulloch, M., Rüggeberg, A. and Eisenhauer, A.: Boron isotope composition of the cold-
889   water coral Lophelia pertusa along the Norwegian margin: Zooming into a potential pH-proxy
890   by combining bulk and high-resolution approaches, Chem. Geol., #pagerange#,
891   doi:10.1016/j.chemgeo.2019.01.005, 2019.

892   Khani, M. H., Pahlavanzadeh, H. and Alizadeh, K.: Biosorption of strontium from aqueous
893   solution by fungus Aspergillus terreus, Environ. Sci. Pollut. Res., 19(6), 2408–2418,
894   doi:10.1007/s11356-012-0753-z, 2012.

895   Kinsman, D.: Trace cations in aragonite, Abstr. Geol. Soc. Am., 2, 596–597, 1970.

896   Kiriakoulakis, K., Fisher, E., Wolff, G. A., Freiwald, A., Grehan, A. and Roberts, J. M.: Lipids
897   and nitrogen isotopes of two deep-water corals from the North-East Atlantic: initial results
898   and implications for their nutrition, in Cold-Water Corals and Ecosystems, pp. 715–729,
899   Springer-Verlag, Berlin/Heidelberg., 2005.

900   Kiriakoulakis, K., Freiwald, A., Fisher, E. and Wolff, G. A.: Organic matter quality and supply
901   to deep-water coral/mound systems of the NW European Continental Margin, Int. J. Earth
902   Sci., 96(1), 159–170, doi:10.1007/s00531-006-0078-6, 2007.

903   Kitano, Y., Okumura, M. and Idogaki, M.: Incorporation of sodium, chloride and sulfate with
904   calcium carbonate., Geochem. J., 9(2), 75–84, doi:10.2343/geochemj.9.75, 1975.

905 Kunioka, D., Shirai, K., Takahata, N., Sano, Y., Toyofuku, T. and Ujiie, Y.: Microdistribution of
906 Mg/Ca, Sr/Ca, and Ba/Ca ratios in Pulleniatina obliquiloculata test by using a NanoSIMS:
907 Implication for the vital effect mechanism, Geochemistry, Geophys. Geosystems, 7(12),
908 doi:10.1029/2006GC001280, 2006.

909 Lear, C., Elderfield, H. and Wilson, P.: Cenozoic {Deep-Sea} Temperatures and Global Ice
910 Volumes from {Mg/Ca} in Benthic Foraminiferal Calcite, Science (80-.)., 287(5451), 269–
911 272, doi:10.1126/science.287.5451.269, 2000.

912 Lewis, E. and Wallace, D. W.: R: Program developed for CO2 system calculations
913 ORNL/CDIAC-105, Carbon Dioxide Inf. Anal. CentreOak Ridge Natl. Lab. US Dep. Energy,
914 Oak Ridge, Tennessee, 1998.

915 Locarnini, R. A., Mishonov, A. V, Antonov, J. I., Boyer, T. P., Garcia, H. E., Baranova, O. K.,
916 Zweng, M. M., Paver, C. R., Reagan, J. R., Johnson, D. R., Hamilton, M., Seidov 1948-, D.
917 and Levitus, S.: World ocean atlas 2013. Volume 1, Temperature, edited by O. C. L. National
918 Oceanographic Data Center (U.S.) and N. E. S. United States Data, and Information
919 Service, , doi:http://doi.org/10.7289/V55X26VD, 2013.

920 López Correa, M., Montagna, P., Vendrell-Simón, B., McCulloch, M. and Taviani, M.: Stable
921 isotopes (δ18O and δ13C), trace and minor element compositions of Recent scleractinians
922 and Last Glacial bivalves at the Santa Maria di Leuca deep-water coral province, Ionian Sea,
923 Deep. Res. Part II Top. Stud. Oceanogr., 57(5–6), 471–486, doi:10.1016/j.dsr2.2009.08.016,
924 2010.

925 Lorens, R. B. and Bender, M. L.: The impact of solution chemistry on Mytilus edulis calcite
926 and aragonite, Geochim. Cosmochim. Acta, 44(9), 1265–1278, doi:10.1016/0016-
927 7037(80)90087-3, 1980.

928 Malone, P. G. and Dodd, J. R.: Temperature and salinity effects on calcification rate in
929 *Mytilus edulis* and its paleoecological implications, Limnol. Oceanogr., 12(3), 432–436,
930 doi:10.4319/lo.1967.12.3.0432, 1967.

931 Marriott, C. S., Henderson, G. M., Belshaw, N. S. and Tudhope, A. W.: Temperature
932 dependence of δ7Li, δ44Ca and Li/Ca during growth of calcium carbonate, Earth Planet. Sci.
933 Lett., 222(2), 615–624, doi:10.1016/j.epsl.2004.02.031, 2004.

934 Marshall, A. T.: Calcification in hermatypic and ahermatypic corals, Science (80-.).,
935 271(5249), 637–639, doi:10.1126/science.271.5249.637, 1996.

936 McConnaughey, T.: 13C and18O isotopic disequilibrium in biological carbonates: I. Patterns,
937 Geochim. Cosmochim. Acta, 53(1), 151–162, doi:10.1016/0016-7037(89)90282-2, 1989.

938 McCulloch, M., Trotter, J., Montagna, P., Falter, J., Dunbar, R., Freiwald, A., Försterra, G.,
939 López Correa, M., Maier, C., Rüggeberg, A. and Taviani, M.: Resilience of cold-water
940 scleractinian corals to ocean acidification: Boron isotopic systematics of pH and saturation
941 state up-regulation, Geochim. Cosmochim. Acta, 87, 21–34, doi:10.1016/j.gca.2012.03.027,
942 2012.

943 van der Meer, M. T. J., Baas, M., Rijpstra, W. I. C., Marino, G., Rohling, E. J., Sinninghe
944 Damsté, J. S. and Schouten, S.: Hydrogen isotopic compositions of long-chain alkenones
945 record freshwater flooding of the Eastern Mediterranean at the onset of sapropel deposition,
946 Earth Planet. Sci. Lett., 262(3–4), 594–600, doi:10.1016/j.epsl.2007.08.014, 2007.

947 Meibom, A., Cuif, J. P., Hillion, F., Constantz, B. R., Juillet-Leclerc, A., Dauphin, Y.,
948 Watanabe, T. and Dunbar, R. B.: Distribution of magnesium in coral skeleton, Geophys. Res.
949 Lett., 31(23), 1–4, doi:10.1029/2004GL021313, 2004.

950 Mertens, K. N., Ribeiro, S., Bouimetarhan, I., Caner, H., Combourieu Nebout, N., Dale, B.,
951 De Vernal, A., Ellegaard, M., Filipova, M., Godhe, A., Goubert, E., Grøsfjeld, K., Holzwarth,

952 U., Kotthoff, U., Leroy, S. A. G., Londeix, L., Marret, F., Matsuoka, K., Mudie, P. J., Naudts,
953 L., Peña-Manjarrez, J. L., Persson, A., Popescu, S. M., Pospelova, V., Sangiorgi, F., van der
954 Meer, M. T. J., Vink, A., Zonneveld, K. A. F., Vercauteren, D., Vlassenbroeck, J. and
955 Louwye, S.: Process length variation in cysts of a dinoflagellate, Lingulodinium
956 machaerophorum, in surface sediments: Investigating its potential as salinity proxy, Mar.
957 Micropaleontol., 70(1–2), 54–69, doi:10.1016/j.marmicro.2008.10.004, 2009.

958 Mezger, E. M., de Nooijer, L. J., Boer, W., Brummer, G. J. A. and Reichart, G. J.: Salinity
959 controls on Na incorporation in Red Sea planktonic foraminifera, Paleoceanography, 31(12),
960 1562–1582, doi:10.1002/2016PA003052, 2016.

961 Mienis, F., de Stigter, H. C., White, M., Duineveld, G., de Haas, H. and van Weering, T. C.
962 E.: Hydrodynamic controls on cold-water coral growth and carbonate-mound development at
963 the SW and SE Rockall Trough Margin, NE Atlantic Ocean, Deep. Res. Part I Oceanogr.
964 Res. Pap., 54(9), 1655–1674, doi:10.1016/j.dsr.2007.05.013, 2007.

965 Mitsuguchi, T., Matsumoto, E., Abe, O., Uchida, T. and Isdale, P. J.: Mg/Ca thermometry in
966 coral skeletons, Science (80-.)., 274(5289), 961–963, doi:10.1126/science.274.5289.961,
967 1996.

968 Mitsuguchi, T., Uchida, T., Matsumoto, E., Isdale, P. J. and Kawana, T.: Variations in Mg/Ca,
969 Na/Ca, and Sr/Ca ratios of coral skeletons with chemical treatments: implications for
970 carbonate geochemistry, Geochim. Cosmochim. Acta, 65(17), 2865–2874,
971 doi:10.1016/S0016-7037(01)00626-3, 2001.

972 Montagna, P., McCulloch, M., Douville, E., López Correa, M., Trotter, J., Rodolfo-Metalpa,
973 R., Dissard, D., Ferrier-Pagès, C., Frank, N., Freiwald, A., Goldstein, S., Mazzoli, C.,
974 Reynaud, S., Rüggeberg, A., Russo, S. and Taviani, M.: Li/Mg systematics in scleractinian
975 corals: Calibration of the thermometer, Geochim. Cosmochim. Acta, 132, 288–310,
976 doi:10.1016/j.gca.2014.02.005, 2014.

977 Mucci, A.: Manganese uptake during calcite precipitation from seawater: Conditions leading
978 to the formation of a pseudokutnahorite, Geochim. Cosmochim. Acta, 52(7), 1859–1868,
979 doi:10.1016/0016-7037(88)90009-9, 1988.

980 Mucci, A. and Morse, J.: Chemistry of low-temperature abiotic calcites: Experimental studies
981 on coprecipitation, stability, and fractionation, Rev. Aquat. Sci, 3(2–3), 217–254, 1990.

982 Neulinger, S. C., Järnegren, J., Ludvigsen, M., Lochte, K. and Dullo, W. C.: Phenotype-
983 specific bacterial communities in the cold-water coral Lophelia pertusa (Scleractinia) and
984 their implications for the coral's nutrition, health, and distribution, Appl. Environ. Microbiol.,
985 74(23), 7272–7285, doi:10.1128/AEM.01777-08, 2008.

986 Okai, T., Suzuki, A., Kawahata, H., Terashima, S. and Imai, N.: Preparation of a New
987 Geological Survey of Japan Geochemical Reference Material: Coral JCp-1, Geostand.
988 Geoanalytical Res., 26(1), 95–99, doi:10.1111/j.1751-908X.2002.tb00627.x, 2002.

989 Okazaki, K.: SKELETON FORMATION OF SEA URCHIN LARVAE. I. EFFECT OF CA
990 CONCENTRATION OF THE MEDIUM, Biol. Bull., 110(3), 320–333, doi:10.2307/1538838,
991 1956.

992 Okumura, M. and Kitano, Y.: Coprecipitation of alkali metal ions with calcium carbonate,
993 Geochim. Cosmochim. Acta, 50(1), 49–58, doi:10.1016/0016-7037(86)90047-5, 1986.

994 Pagliarani, A., Bandiera, P., Ventrella, V., Trombetti, F., Pirini, M. and Borgatti, A. R.:
995 Response to alkyltins of two Na+-dependent ATPase activities in Tapes philippinarum and
996 Mytilus galloprovincialis, Toxicol. Vitr., 20(7), 1145–1153, doi:10.1016/j.tiv.2006.02.006,
997 2006.

998 Pytkowicz, R. M. and Conners, D. N.: High pressure solubility of calcium carbonate in

999   seawater, Science (80-.)., 144(3620), 840–841, doi:10.1126/science.144.3620.840, 1964.

1000   Raddatz, J., Liebetrau, V., Rüggeberg, A., Hathorne, E., Krabbenhöft, A., Eisenhauer, A.,
1001   Böhm, F., Vollstaedt, H., Fietzke, J., Correa, M. L., Freiwald, A. and Dullo, W.: Stable Sr-
1002   isotope , Sr / Ca , Mg / Ca , Li / Ca and Mg / Li ratios in the scleractinian cold-water coral
1003   Lophelia pertusa, Chem. Geol., 352, 143–152, doi:10.1016/j.chemgeo.2013.06.013, 2013.

1004   Raddatz, J., Rüggeberg, A., Liebetrau, V., Foubert, A., Hathorne, E. C., Fietzke, J.,
1005   Eisenhauer, A. and Dullo, W. C.: Environmental boundary conditions of cold-water coral
1006   mound growth over the last 3 million years in the Porcupine Seabight, Northeast Atlantic,
1007   Deep. Res. Part II Top. Stud. Oceanogr., 99, 227–236, doi:10.1016/j.dsr2.2013.06.009,
1008   2014a.

1009   Raddatz, J., Rüggeberg, A., Flögel, S., Hathorne, E. C., Liebetrau, V., Eisenhauer, A. and
1010   Dullo, W. C.: The influence of seawater pH on U/Ca ratios in the scleractinian cold-water
1011   coral Lophelia pertusa, Biogeosciences, 11(7), 1863–1871, doi:10.5194/bg-11-1863-2014,
1012   2014b.

1013   Raddatz, J., Liebetrau, V., Trotter, J., Rüggeberg, A., Flögel, S., Dullo, W. C., Eisenhauer, A.,
1014   Voigt, S. and McCulloch, M.: Environmental constraints on Holocene cold-water coral reef
1015   growth off Norway: Insights from a multiproxy approach, Paleoceanography, 31(10), 1350–
1016   1367, doi:10.1002/2016PA002974, 2016.

1017   Ragland, P. C., Pilkey, O. H. and Blackwelder, B. W.: Diagenetic changes in the elemental
1018   composition of unrecrystallized mollusk shells, Chem. Geol., 25(1–2), 123–134,
1019   doi:10.1016/0009-2541(79)90088-3, 1979.

1020   Ramos, A. A., Inoue, Y. and Ohde, S.: Metal contents in Porites corals: Anthropogenic input
1021   of river run-off into a coral reef from an urbanized area, Okinawa, Mar. Pollut. Bull., 48(3–4),
1022   281–294, doi:10.1016/j.marpolbul.2003.08.003, 2004.

1023   Roberts, J. M.: Reefs of the Deep: The Biology and Geology of Cold-Water Coral
1024   Ecosystems, Science (80-.)., 312(5773), 543–547, doi:10.1126/science.1119861, 2006.

1025   Roberts, J. M., Wheeler, A., Freiwald, A. and Cairns, S.: Cold-Water Corals, Cambridge
1026   University Press, Cambridge., 2009.

1027   Robinson, L. F., Adkins, J. F., Frank, N., Gagnon, A. C., Prouty, N. G., Brendan Roark, E.
1028   and de Flierdt, T. van: The geochemistry of deep-sea coral skeletons: A review of vital
1029   effects and applications for palaeoceanography, Deep. Res. Part II Top. Stud. Oceanogr.,
1030   99, 184–198, doi:10.1016/j.dsr2.2013.06.005, 2014.

1031   Roder, C., Berumen, M. L., Bouwmeester, J., Papathanassiou, E., Al-Suwailem, A. and
1032   Voolstra, C. R.: First biological measurements of deep-sea corals from the Red Sea, Sci.
1033   Rep., 3(1), 2802, doi:10.1038/srep02802, 2013.

1034   Rollion-Bard, C. and Blamart, D.: SIMS method and examples of applications in coral
1035   biomineralization, Biominer. Sourceb., (March), 249–261, doi:10.1201/b16621-20, 2014.

1036   Rollion-Bard, C. and Blamart, D.: Possible controls on Li, Na, and Mg incorporation into
1037   aragonite coral skeletons, Chem. Geol., 396, 98–111, doi:10.1016/j.chemgeo.2014.12.011,
1038   2015.

1039   Rollion-Bard, C., Blamart, D., Cuif, J. P. and Dauphin, Y.: In situ measurements of oxygen
1040   isotopic composition in deep-sea coral, Lophelia pertusa: Re-examination of the current
1041   geochemical models of biomineralization, Geochim. Cosmochim. Acta, 74(4), 1338–1349,
1042   doi:10.1016/j.gca.2009.11.011, 2010.

1043   Rollion-Bard, C., Blamart, D., Trebosc, J., Tricot, G., Mussi, A. and Cuif, J. P.: Boron isotopes
1044   as pH proxy: A new look at boron speciation in deep-sea corals using11B MAS NMR and
1045   EELS, Geochim. Cosmochim. Acta, 75(4), 1003–1012, doi:10.1016/j.gca.2010.11.023, 2011.

1046 Rosenthal, Y., Field, M. P. and Sherrell, R. M.: Precise Determination of Element/Calcium
1047 Ratios in Calcareous Samples Using Sector Field Inductively Coupled Plasma Mass
1048 Spectrometry, Anal. Chem., 71(15), 3248–3253, doi:10.1021/ac981410x, 1999.

1049 Rucker, J. B. and Valentine, J. W.: Salinity response of trace element concentration in
1050 Crassostrea virginica, Nature, 190(4781), 1099–1100, doi:10.1038/1901099a0, 1961.

1051 Rüggeberg, A., Flögel, S., Dullo, W. C., Hissmann, K. and Freiwald, A.: Water mass
1052 characteristics and sill dynamics in a subpolar cold-water coral reef setting at Stjernsund,
1053 northern Norway, Mar. Geol., 282(1–2), 5–12, doi:10.1016/j.margeo.2010.05.009, 2011.

1054 Ruiz-Hernandez, S. E., Grau-Crespo, R., Almora-Barrios, N., Wolthers, M., Ruiz-Salvador, A.
1055 R., Fernandez, N. and De Leeuw, N. H.: Mg/Ca partitioning between aqueous solution and
1056 aragonite mineral: A molecular dynamics study, Chem. - A Eur. J., 18(32), 9828–9833,
1057 doi:10.1002/chem.201200966, 2012.

1058 Schouten, S., Ossebaar, J., Schreiber, K., Kienhuis, M. V. M., Langer, G., Benthien, A. and
1059 Bijma, J.: The effect of temperature, salinity and growth rate on the stable hydrogen isotopic
1060 composition of long chain alkenones produced by Emiliania huxleyi and Gephyrocapsa
1061 oceanica, Biogeosciences, 3(1), 113–119, doi:10.5194/bg-3-113-2006, 2006.

1062 Sevilgen, D. S., Venn, A. A., Hu, M. Y., Tambutté, E., de Beer, D., Planas-Bielsa, V. and
1063 Tambutté, S.: Full in vivo characterization of carbonate chemistry at the site of calcification in
1064 corals, Sci. Adv., 5(1), eaau7447, doi:10.1126/sciadv.aau7447, 2019.

1065 Shelton, G. A. B.: LOPHELIA pertusa (l.): Electrical conduction and behaviour in a deep-
1066 water coral, J. Mar. Biol. Assoc. United Kingdom, 60(2), 517–528,
1067 doi:10.1017/S0025315400028538, 1980.

1068 Shirai, K., Kusakabe, M., Nakai, S., Ishii, T., Watanabe, T., Hiyagon, H. and Sano, Y.: Deep-
1069 sea coral geochemistry: Implication for the vital effect, Chem. Geol., 224(4), 212–222,
1070 doi:10.1016/j.chemgeo.2005.08.009, 2005.

1071 Sinclair, D. J., Williams, B. and Risk, M.: A biological origin for climate signals in corals -
1072 Trace element "vital effects" are ubiquitous in Scleractinian coral skeletons, Geophys. Res.
1073 Lett., 33(17), 1–5, doi:10.1029/2006GL027183, 2006.

1074 Sizer, I. W.: Effects of temperature on enzyme kinetics, in Advances in Enzymology and
1075 Related Areas of Molecular Biology, pp. 35–62, Wiley-Blackwell., 2006.

1076 Stolarski, J.: Three-dimensional micro- and nanostructural characteristics of the scleractinian
1077 coral skeleton: A biocalcification proxy, Acta Palaeontol. Pol., 48(4), 497–530, doi:Available
1078 from: http://www.app.pan.pl/article/item/app48-497.html., 2003.

1079 Swart, P. K.: The strontium, magnesium and sodium composition of recent scleractinian coral
1080 skeletons as standards for palaeoenvironmental analysis, Palaeogeogr. Palaeoclimatol.
1081 Palaeoecol., 34(C), 115–136, doi:10.1016/0031-0182(81)90060-2, 1981.

1082 Tambutté, E., Allemand, D., Zoccola, D., Meibom, A., Lotto, S., Caminiti, N. and Tambutté,
1083 S.: Observations of the tissue-skeleton interface in the scleractinian coral Stylophora
1084 pistillata, Coral Reefs, 26(3), 517–529, doi:10.1007/s00338-007-0263-5, 2007.

1085 Tambutté, S., Holcomb, M., Ferrier-Pagès, C., Reynaud, S., Tambutté, É., Zoccola, D. and
1086 Allemand, D.: Coral biomineralization: From the gene to the environment, J. Exp. Mar. Bio.
1087 Ecol., 408(1–2), 58–78, doi:10.1016/j.jembe.2011.07.026, 2011.

1088 Taviani, M., Remia, A., Corselli, C., Freiwald, A., Malinverno, E., Mastrototaro, F., Savini, A.
1089 and Tursi, A.: First geo-marine survey of living cold-water Lophelia reefs in the Ionian Sea
1090 (Mediterranean basin), Facies, 50(3–4), 409–417, doi:10.1007/s10347-004-0039-0, 2005.

1091 Trivedi, B. and Danforth, W. H.: Effect of pH on the kinetics of frog muscle

1092   phosphofructokinase., J. Biol. Chem., 241(17), 4110–4112, doi:10.2196/jmir.1752, 1966.

1093   Turekian, K. K., Steele, J. H. and Thorpe, S. A.: Marine Chemistry & Geochemistry A
1094   DERIVATIVE OF ENCYCLOPEDIA OF OCEAN SCIENCES., 2010.

1095   de Villiers, S., Shen, G. T. and Nelson, B. K.: The Sr/Ca-temperature relationship in coralline
1096   aragonite: Influence of variability in (Sr/Ca)Seawater and skeletal growth parameters,
1097   Geochim. Cosmochim. Acta, 58(1), 197–208, doi:10.1016/0016-7037(94)90457-X, 1994.

1098   Wang, K., Villalobo, A. and Roufogalis, B.: The plasma membrane calcium pump: a
1099   multiregulated transporter, Trends Cell Biol., 2(February), 46–52 [online] Available from:
1100   http://www.ncbi.nlm.nih.gov/pubmed/14731526 (Accessed 22 August 2018), 1992.

1101   Wang, W. X. and Fisher, N. S.: Effects of calcium and metabolic inhibitors on trace element
1102   uptake in two marine bivalves, J. Exp. Mar. Bio. Ecol., 236(1), 149–164, doi:10.1016/S0022-
1103   0981(98)00195-6, 1999.

1104   Watson, E. B.: WATSON - surface enrichment and trace-element uptake during crystal
1105   growth, , 60(24), 5013–5020, 1996.

1106   Weldeab, S., Lea, D. W., Schneider, R. R. and Andersen, N.: Centennial scale climate
1107   instabilities in a wet early Holocene West African monsoon, Geophys. Res. Lett., 34(24), 1–
1108   6, doi:10.1029/2007GL031898, 2007.

1109   White, A. F.: Sodium and potassium coprecipitation in aragonite, Geochim. Cosmochim.
1110   Acta, 41(5), 613–625, doi:10.1016/0016-7037(77)90301-5, 1977.

1111   Wit, J. C., De Nooijer, L. J., Wolthers, M. and Reichart, G. J.: A novel salinity proxy based on
1112   na incorporation into foraminiferal calcite, Biogeosciences, 10(10), 6375–6387,
1113   doi:10.5194/bg-10-6375-2013, 2013.

1114   Yamazato, K.: Calcification in a solitary coral, Fungia scutaria Lamarck in relation to
1115   environmental factors, 1966.

1116   Yoshimura, T., Tamenori, Y., Suzuki, A., Kawahata, H., Iwasaki, N., Hasegawa, H., Nguyen,
1117   L. T., Kuroyanagi, A., Yamazaki, T., Kuroda, J. and Ohkouchi, N.: Altervalent substitution of
1118   sodium for calcium in biogenic calcite and aragonite, Geochim. Cosmochim. Acta, 202, 21–
1119   38, doi:10.1016/j.gca.2016.12.003, 2017.

1120   Zeebe, R. E. and Wolf-Gladrow, D. A.: CO2 in seawater : equilibrium, kinetics, isotopes.
1121   [online] Available from: http://epic.awi.de/4276/ (Accessed 22 August 2018), 2001.

1122   Zonneveld, K. A. F., P. Hoek, R., Brinkhuis, H. and Helmut Willems: Geographical
1123   distributions of organic-walled dinoflagellate cysts in surficial sediments of the Benguela
1124   upwelling region and their relationship to upper ocean conditions, Prog. Oceanogr., 48(1),
1125   25–72, doi:10.1016/S0079-6611(00)00047-1, 2001.

1126   Zweng, M. M., Reagan, J. R., Antonov, J. I., Locarnini, R. A., Mishonov, A. V, Boyer, T. P.,
1127   Garcia, H. E., Baranova, O. K., Johnson, D. R., Seidov 1948-, D., Biddle, M. M. and Levitus,
1128   S.: World ocean atlas 2013. Volume 2, Salinity, edited by O. C. L. National Oceanographic
1129   Data Center (U.S.) and N. E. S. United States Data, and Information Service, ,
1130   doi:http://doi.org/10.7289/V5251G4D, 2013.

1131   Zweng, M. M., Reagan, J. R., Antonov, J. I., Locarnini, R. A., Mishonov, A. V, Boyer, T. P.,
1132   Garcia, H. E., Baranova, O. K., Johnson, D. R., Seidov 1948-, D., Biddle, M. M. and Levitus,
1133   S.: World ocean atlas 2013. Volume 2, Salinity, edited by O. C. L. National Oceanographic
1134   Data Center (U.S.) and N. E. S. United States Data, and Information Service, ,
1135   doi:http://doi.org/10.7289/V5251G4D, 2013.

1136